AD-A111 873 NAVAL SURFACE WEAPONS CENTER SILVER SPRING MD F/G 20/7
STABILITY PROPERTIES OF AN INTENSE RELATIVISTIC NONNEUTRAL ELEC--ETC(U)
SEP 81 H S UHM, R C DAVIDSON
UNCLASSIFIED NSWC/TR-81-389 SBI-AD-F500 003 NL

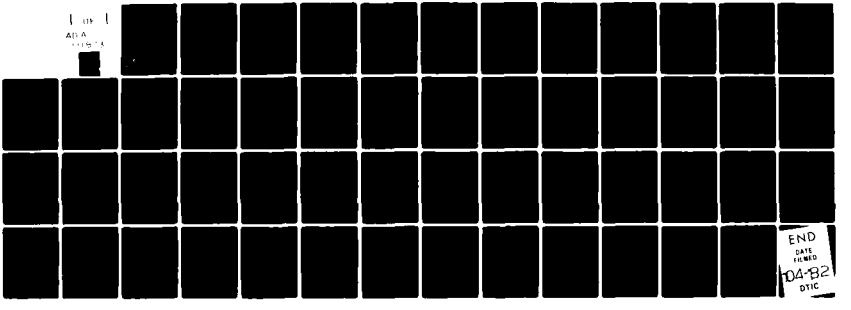

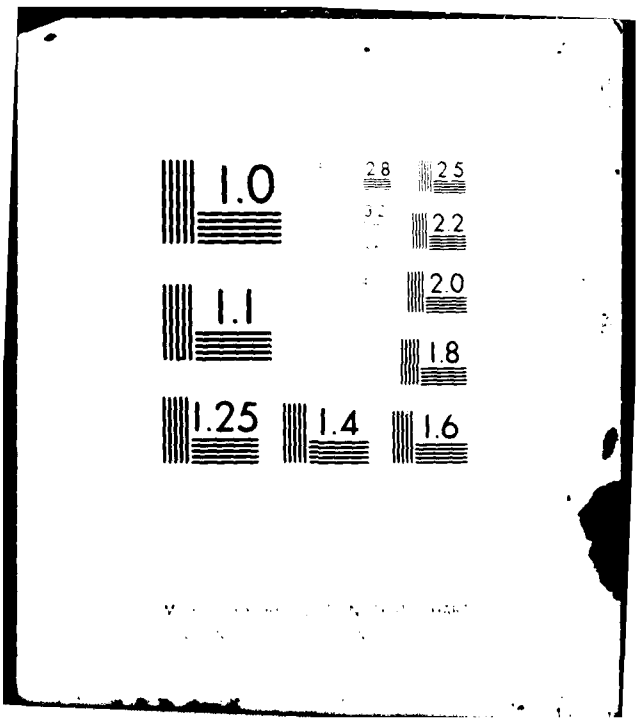
1.0
2.8
2.5
2.2
2.0
1.1
1.8
1.25
1.4
1.6

NSWC TR 81-389

STABILITY PROPERTIES OF AN INTENSE RELATIVISTIC NONNEUTRAL ELECTRON RING IN A MODIFIED BETATRON ACCELERATOR

BY HANS S. UHM RONALD C. DAVIDSON

RESEARCH AND TECHNOLOGY DEPT.

SEPTEMBER 1981

NAVAL SURFACE WEAPONS CENTER

Dahlgren, Virginia 22448 • Silver Spring, Maryland 20910

UNCLASSIFIED

SECURITY CLASSIFICATION OF THIS PAGE (When Data Entered)

REPORT DOCUMENTATION PAGE	READ INSTRUCTIONS BEFORE COMPLETING FORM
1. REPORT NUMBER: NSWC TR 81-389	2. GOVT ACCESSION NO.: AD A111 873
3. RECIPIENT'S CATALOG NUMBER:	
4. TITLE (and Subtitle): Stability Properties of an Intense Relativistic Nonneutral Electron Ring in a Modified Betatron Accelerator	5. TYPE OF REPORT & PERIOD COVERED: Final
	6. PERFORMING ORG. REPORT NUMBER:
7. AUTHOR(s): Ronald C. Davidson and Han S. Uhm	8. CONTRACT OR GRANT NUMBER(s):
9. PERFORMING ORGANIZATION NAME AND ADDRESS: Naval Surface Weapons Center, R41, White Oak, Silver Spring, Maryland	10. PROGRAM ELEMENT, PROJECT, TASK AREA & WORK UNIT NUMBERS: 61152N, ZR00001, ZR01109, 0
11. CONTROLLING OFFICE NAME AND ADDRESS:	12. REPORT DATE: September 1981
	13. NUMBER OF PAGES: 54
14. MONITORING AGENCY NAME & ADDRESS(if different from Controlling Office):	15. SECURITY CLASS. (of this report): UNCLASSIFIED
	15a. DECLASSIFICATION/DOWNGRADING SCHEDULE:

16. DISTRIBUTION STATEMENT (of this Report)

Approved for public release, distribution unlimited

17. DISTRIBUTION STATEMENT (of the abstract entered in Block 20, if different from Report)

18. SUPPLEMENTARY NOTES

19. KEY WORDS (Continue on reverse side if necessary and identify by block number)

Modified Betatron
Nonneutral Electron Ring
Intense Relativistic Beam
Negative-Mass Instability

20. ABSTRACT (Continue on reverse side if necessary and identify by block number)

Equilibrium and stability properties of an intense electron ring located at the midplane of an externally applied mirror field are investigated within the framework of the linearized Vlasov-Maxwell equations, including the important influence of equilibrium self fields and an applied field $B_{0\theta}$ in the toroidal direction. It is assumed that the ring is thin and that $\nu/\gamma_b \ll 1$, where ν is Budker's parameter and $\gamma_b mc^2$ is the characteristic electron energy. Equilibrium and stability properties are calculated for the choice of equilibrium distribution function in which all electrons have the same value

DD FORM 1 JAN 73 1473 EDITION OF 1 NOV 65 IS OBSOLETE
S/N 0102-014-6601

UNCLASSIFIED
SECURITY CLASSIFICATION OF THIS PAGE (When Data Entered)

of energy in a frame of reference rotating with angular velocity ω_b in the minor cross section of the ring, and a Lorentzian distribution in canonical angular momentum P_θ. Negative-mass and resistive-wall stability properties are calculated, and a closed dispersion relation is obtained for the case where the ring is located inside a toroidal conductor with finite resistivity and minor radius a_c much less than the major radius R_c. One of the most important features of the stability analysis is that the negative-mass instability in a high-current ring can be stabilized by equilibrium self-field effects in circumstances where the self fields are sufficiently intense. Moreover, a modest spread Δ in canonical angular momentum can stabilize the resistive-wall instability.

CONTENTS

ILLUSTRATIONS

FOREWORD

Equilibrium and stability properties of an intense electron ring located at the midplane of an externally applied mirror field are investigated within the framework of the linearized Vlasov-Maxwell equations, including the important influence of equilibrium self fields and an applied field $B_{0\theta}^{ext}$ in the toroidal direction. It is assumed that the ring is thin and that $\nu/\gamma_b << 1$, where ν is Budker's parameter and $\gamma_b mc^2$ is the characteristic electron energy. Equilibrium and stability properties are calculated for the choice of equilibrium distribution function in which all electrons have the same value of energy in a frame of reference rotating with angular velocity ω_b in the minor cross section of the ring, and a Lorentzian distribution in canonical angular momentum P_θ. Negative-mass and resistive-wall stability properties are calculated, and a closed dispersion relation is obtained for the case where the ring is located inside a toroidal conductor with finite resistivity and minor radius a_c much less than the major radius R_0. One of the most important features of the stability analysis is that the negative-mass instability in a high-current ring can be stabilized by equilibrium self-field effects in circumstances where the self fields are sufficiently intense. Moreover, a modest spread Δ in canonical angular momentum can stabilize the resistive-wall instability.

Ira M Blatstein

IRA M. BLATSTEIN
By direction

INTRODUCTION

There is considerable recent interest in the equilibrium and stability properties of intense relativistic electron rings with applications that include high-current betatron accelerators.[1-4] In a conventional betatron accelerator, a toroidal electron ring is confined in a mirror or betatron magnetic field. Moreover, the beam density and current is limited by the strength of the betatron magnetic field. In the modified betatron accelerator,[1,2] however, an additional confining magnetic field $B_{0\theta}^{ext}$ is applied in the toroidal direction, thereby considerably increasing the limiting beam current and density. In the present article, we make use of the Vlasov-Maxwell equations to investigate the equlibrium and stability properties[5-10] of an intense relativistic electron ring confined in a modified betatron field configuration,[1,2] including the important influence of equilibrium self-field effects and the toroidal magnetic field $B_{0\theta}^{ext}$. The analysis is carried out for an electron ring located at the midplane of an externally applied mirror field. The positive ions form an immobile ($m_i \rightarrow \infty$) background that provides partial charge neutralization. In addition, it is assumed that the electron ring has minor dimensions much smaller than the major radius R_0 (Fig. 1). It is also assumed that $\nu/\gamma_b << 1$, where ν is Budker's parameter and $\gamma_b mc^2$ is the characteristic electron energy associated with the toroidal motion.

Equilibrium and stability properties are calculated for the specific choice of the equilibrium electron distribution function [Eq. (13)]

$$f_b^0(H,P_\phi,P_\theta) = \frac{\hat{n}_b R_0 \Delta}{2\pi^2 \gamma_b m} \frac{\delta(H - \omega_b P_\phi - \hat{\gamma} mc^2)}{[(P_\theta - P_0)^2 + \Delta^2]}$$

where H is the energy, P_θ is the canonical angular momentum in the azimuthal direction, $P_\phi = \rho p_\phi - e\hat{B}_\theta \rho^2/2c$ is the canonical angular momentum in the small cross section of the torus, R_0 is the major radius of the ring, and $\hat{n}_b$, Δ, P_0, ω_b and $\hat{\gamma}$ are constants. Although H and P_θ are exact single-particle invariants for the equilibrium configuration illustrated in Fig. 1, P_ϕ is an approximate invariant whenever the toroidal field is sufficiently strong [Eq. (8)] and the electron ring has circular cross section (Appendix A) with

$$n = \frac{1}{2} \text{ and } a = b \ .$$

Here $n = -[r(\partial/\partial r)\ell n B_{0z}^{ext}(r,z)]_{(R_0,0)}$ is the external field index. Equilibrium properties[8,9] of the electron ring are calculated in Section II. One of the most important features of the equilibrium analysis is that the maximum electron density trapped in the ring can be greatly enhanced by the toroidal magnetic field [Eqs. (43) and (44)]. Moreover, the rotation frequency ω_b in the minor cross section of the ring plays an important role in determining detailed equilibrium properties.

The formal electromagnetic stability analysis is carried out in Section III within the framework of the linearized Vlasov-Maxwell equations. Negative-mass and resistive-wall stability properties[5-7,10] are calculated for eigenfrequency ω near harmonics of the cyclotron frequency $\omega_{cz} = eB_{0z}^{ext}(R_0,0)/\gamma_b mc$ associated with the axial magnetic field, i.e., $\omega \simeq \ell\omega_{cz}$. The resulting dispersion relation in Eq. (77) is obtained analytically for a relativistic electron ring located inside a toroidal conductor with finite resistivity and minor radius a_c. Equation (77) is one of the main results of this paper and can be used to investigate stability properties for a broad range of physical parameters.

Negative-mass stability properties[5-7,10] are investigated in Section IV, assuming a perfectly conducting wall but including the important influence of equilibrium self fields. Introducing the parameter [Eq. (64)]

$$\mu = \omega_{cz}^2/\omega_\beta^2 - 1/\gamma_b^2 ,$$

we find that [Eq. (88)]

$$0 < \mu < \frac{\nu}{\gamma_b}\left(\frac{mR_0c}{e}\right)^2 g$$

is a necessary and sufficient condition for instability. Here, g is a geometric factor with $g = (1 + 2\ell n a_c/a)$ for $a_c >> a$ and $g = 4/\lambda_{0n}^2$ for $a_c \simeq a$, where $J_0(\lambda_{0n}) = 0$. Moreover, $\omega_\beta^2 = \omega_{cz}^2/2 + (\omega_{pb}^2/2)[\beta_b^2 - (1 - f)]$ is the radial betatron frequency-squared for a circular beam with a = b and n = 1/2, $\omega_{pb}^2 = 4\pi\hat{n}_b e^2/\gamma_b m$ is the relativistic plasma frequency-squared, and f is the fractional charge neutralization. Evidently, from Eqs. (64) and (88), equilibrium self fields can have a large influence on stability behavior. Moreover, the negative-mass instability can be completely stabilized by a sufficiently large spread Δ in canonical angular momentum P_θ.

It is also important to note that $\mu < 0$ is a sufficient condition for stability (Section IV) even with zero spread in canonical angular momentum ($\Delta = 0$). The condition $\mu < 0$ can be satisfied provided the equilibrium self fields are sufficiently strong in absolute intensity. For example, if f = 0, then the sufficient condition for stability ($\mu < 0$) and existence of a confined equilibrium [Eq. (44)] can be expressed as $1 < \omega_{pb}^2/\gamma_b^2\omega_{cz}^2 < 1 + \omega_{c\theta}^2/2\omega_{cz}^2$.

Although a perfect conducting wall is a reasonable assumption in many experiments, we expect a significant modification of stability behavior when a small amount of resistivity is introduced into the wall, e.g., to stabilize the transverse precession in the minor cross section of the ring.

In this regard, in Section V, we investigate the resistive-wall instability[5] assuming that $\mu < 0$ and the negative-mass instability is absent. It is shown that the resistive-wall instability can also be stabilized by a modest spread Δ in the canonical angular momentum.

EQUILIBRIUM CONFIGURATION AND BASIC ASSUMPTIONS

A. Basic Assumptions

The equilibrium configuration is illustrated in Fig. 1. It consists of a relativistic electron ring located at the midplane of an applied focussing (mirror) field $B_{0r}^{ext}(r,z)\hat{e}_r + B_{0z}^{ext}(r,z)\hat{e}_z$. In addition, the electron ring is located inside a toroidal conductor with minor radius a_c. The applied toroidal magnetic field $B_{0\theta}^{ext}\hat{e}_\theta$, where

$$B_{0\theta}^{ext} = \hat{B}_\theta \frac{R_0}{r} , \tag{1}$$

together with the mirror field act to confine the ring both axially and radially. Here, $\hat{e}_r$, $\hat{e}_\theta$, and $\hat{e}_z$ are unit vectors in the r-, θ-, and z-directions, respectively. The equilibrium radius of the ring is denoted by R_0, and the minor dimensions of the ring are denoted by 2a (radial dimension) and 2b (axial dimension). In addition to the cylindrical polar coordinates (r,θ,z), we also introduce the toroidal polar coordinate system (ρ,ϕ,θ) illustrated in Fig. 1 and defined by

$$r - R_0 \equiv r' = \rho\cos\phi ,$$

$$z = \rho\sin\phi , \tag{2}$$

where ρ is measured from the equilibrium radius R_0. The electrons composing the ring undergo a large orbit gyration in the external mirror field with characteristic mean azimuthal velocity $V_\theta^0 = \beta_b c$ in the positive θ-direction. The associated ring current, which is in the negative θ-direction, produces a self-magnetic field $B_0^s(x)$ that threads the ring in the sense indicated in Fig. 1. This self-magnetic field acts as a focussing field which tends to confine the ring electrons

both axially and radially. The electron ring is assumed to be partially charge neutralized by a positive ion background. The excess electrons form a potential well for the ions. For the electrons, however, the self-electric field is defocussing, i.e., in the direction of increasing the minor dimensions of the ring.

To make the theoretical analysis tractable, we make the following simplifying assumptions in describing the electron ring equilibrium by the steady-state Vlasov-Maxwell equations.[8,9]

(a) The positive ions form an immobile ($m_i \to \infty$) partially neutralizing background. The equilibrium ion density $n_i^0(r,z)$ and electron density $n_e^0(r,z)$ are assumed to be related by

$$n_i^0(r,z) = f n_e^0(r,z) \ , \tag{3}$$

where f = const. is the fractional charge neutralization.

(b) The minor dimensions of the ring are much smaller than its major radius, i.e.,

$$a,b \ll R_0 \ . \tag{4}$$

To further simplify the analysis we also assume that the minor cross section of the ring is circular with

$$a = b \ , \tag{5}$$

which is consistent (strictly speaking) provided the external field index n satisfies

$$n = 1/2 \ , \tag{6}$$

where $n = -[r\partial \ell n B_{0z}^{ext}(r,z)/\partial r]_{(R_0,0)}$.

(d) Consistent with Eq. (4), it is also assumed that the transverse (r,z) kinetic energy of an electron is small in comparison with the characteristic azimuthal energy $\gamma_b mc^2$, i.e.,

$$\frac{1}{2\gamma_b m}(p_r^2 + p_z^2) << \gamma_b mc^2 , \tag{7}$$

where $p_\theta \approx \gamma_b m\beta_b c$ is the characteristic azimuthal momentum.

(e) The maximum spread in canonical angular momentum δP_θ is assumed to be small with $|\delta P_\theta| << \gamma_b m\beta_b cR_0$ and

$$\frac{|\delta P_\theta|}{\gamma_b m\beta_b cR_0} << \frac{\hat{B}_\theta}{\hat{B}_z}\left|\frac{p_\perp}{p_\theta}\right| . \tag{8}$$

Here, $p_\perp = (p_r^2 + p_z^2)^{1/2}$ is the characteristic transverse (r,z) momentum, $p_\theta \approx \gamma_b m\beta_b c$ is the characteristic azimuthal momentum, and $\hat{B}_\theta \equiv B_{0\theta}^{ext}(R_0,0)$ and $\hat{B}_z = B_{0z}^{ext}(R_0,0)$. Moreover, $\delta P_\theta \equiv P_\theta - P_0$, where P_θ is the canonical angular momentum, and P_0 = const. is the average canonical angular momentum of the electrons composing the ring. As shown in Appendix A, the inequality in Eq. (8) (which is satisfied provided the spread in canonical angular momentum δP_θ is sufficiently small and/or the toroidal field $\hat{B}_\theta$ is sufficiently strong), together with Eqs. (5) and (6) are sufficient to assure that the canonical angular momentum $P_\phi = \rho p_\phi - (e\hat{B}_\theta/2c)\rho^2$ defined in the small cross-section of the torus is a good approximate invariant.

(f) It is further assumed that

$$\frac{\nu}{\gamma_b} = \frac{N_e}{2\pi R_0}\frac{e^2}{mc^2}\frac{1}{\gamma_b} << 1 , \tag{9}$$

where $\nu = (N_e/2\pi R_0)(e^2/mc^2)$ is Budker's parameter, N_e is the total number of electrons in the ring, and e^2/mc^2 is the classical electron radius. While Eq. (9) assures that the equilibrium self fields E_{0r}^s, E_{0z}^s, B_{0z}^s, and B_{0r}^s are weak in absolute intensity (in comparison

with B_{0z}^{ext}), depending on the beam density we will find that the self-field gradients can be large and have a correspondingly large influence on particle orbits in the equilibrium field configuration.[8,9]

B. Self-Consistent Vlasov Equilibrium

For azimuthally symmetric equilibria ($\partial/\partial\theta = 0$) with both r and z dependence, there are two exact single-particle constants of the motion. These are the total energy H,

$$H = (m^2c^4 + c^2\underset{\sim}{p}^2)^{1/2} - e\phi_0(r,z) \ , \tag{10}$$

and the canonical angular momentum P_θ,

$$P_\theta = r[p_\theta - \frac{e}{c} A_\theta^0(r,z)] \ , \tag{11}$$

where $\underset{\sim}{p} = \gamma m \underset{\sim}{v}$ is the mechanical momentum, $\phi_0(r,z)$ is the equilibrium electrostatic potential, -e is the electron charge, c is the speed of light in vacuo, m is the electron rest mass, and $A_\theta^0(r,z) = A_{0\theta}^{ext}(r,z) + A_{0\theta}^{s}(r,z)$ is the θ-component of the vector potential for the total (external plus self) equilibrium magnetic field. Without loss of generality, we assume $\phi_0(R_0,0) = A_{0\theta}^{s}(R_0,0) = 0$ in Eqs. (10) and (11). Within the context of Eqs. (3) - (9), it is shown in Appendix A that the canonical angular momentum P_ϕ

$$P_\phi = \rho p_\phi - \frac{e}{2c} \hat{B}_\theta \rho^2 \ , \tag{12}$$

in the plane perpendicular to the toroidal magnetic field $B_{0\theta}^{ext}$ is an approximate single-particle invariant for a thin circular beam with a = b and n = 1/2. Here, p_ϕ is the mechanical momentum in the ϕ-direction [Fig. 1], and $\rho^2 = (r - R_0)^2 + z^2$ is defined in Eq. (2). In obtaining

Eq. (12), the toroidal magnetic field $B_{0\theta}^{ext} = \hat{B}_\theta R_0/r$ has been approximated as uniform over the minor cross section of the ring.

Any distribution function f_b^0 that is a function only of the single-particle constants of the motion in the equilibrium field configuration satisfies the steady-state ($\partial/\partial t = 0$) Vlasov equation. For present purposes, we consider the electron distribution function specified by

$$f_b^0(H,P_\phi,P_\theta) = \frac{\hat{n}_b R_0 \Delta}{2\pi^2 \gamma_b m} \frac{\delta(H - \omega_b P_\phi - \hat{\gamma} mc^2)}{(P_\theta - P_0)^2 + \Delta^2} , \tag{13}$$

where $\hat{n}_b = n_b^0(R_0,0)$ is the electron density at the equilibrium radius $(r,z) = (R_0,0)$, ω_b = const. is the angular velocity of mean rotation in the ϕ-direction, Δ is the characteristic spread in the canonical angular momentum P_θ, and $\hat{\gamma}$ is a constant.

The equilibrium Poisson equation can be expressed as

$$\left(\frac{1}{r}\frac{\partial}{\partial r} r \frac{\partial}{\partial r} + \frac{\partial^2}{\partial z^2}\right)\phi_0(r,z) = 4\pi e(1-f)\int d^3p\, f_b^0(H,P_\phi,P_\theta) . \tag{14}$$

Furthermore, the θ-component of the $\nabla \times \underset{\sim}{B}_0^s(\underset{\sim}{x})$ Maxwell equation can be expressed as

$$\left(\frac{\partial}{\partial r}\frac{1}{r}\frac{\partial}{\partial r} r + \frac{\partial^2}{\partial z^2}\right)A_{0\theta}^s(r,z) = \frac{4\pi e}{c}\int d^3p\, v_\theta\, f_b^0(H,P_\phi,P_\theta) , \tag{15}$$

where $v_\theta = (p_\theta/m)(1 + \underset{\sim}{p}^2/m^2c^2)^{-1/2}$ is the azimuthal electron velocity.

Consistent with the thin ring approximation [Eq. (4)] is the requirement that the r-z kinetic energy be small in comparison with the effective azimuthal energy [Eq. (7)]

$$\gamma_\theta(r,z)mc^2 = \left\{ m^2c^4 + c^2 \left[\frac{P_0}{r} + \frac{e}{c} A_\theta^0(r,z) \right]^2 \right\}^{1/2} , \tag{16}$$

defined for $p_\perp^2 = p_r^2 + p_z^2 = 0$ and $P_\theta = P_0$, and that the spread in canonical angular momentum be small with $|\delta P_\theta| = |P_\theta - P_0| \ll \gamma_b m \beta_b c R_0$. Taylor expanding for small values of $p_r^2 + p_z^2$ and $\delta P_\theta = P_\theta - P_0$, we find that the total energy H defined in Eq. (10) can be approximated by[7-10]

$$H = \frac{p_r^2 + p_z^2}{2\gamma_\theta(r,z)m} + \gamma_\theta(r,z)mc^2 - e\phi_0(r,z) + \frac{V_\theta^0(r,z)}{r}(\delta P_\theta) + \frac{(\delta P_\theta)^2}{2\gamma_\theta^3(r,z)mr^2} , \tag{17}$$

where the mean azimuthal velocity of an electron fluid element $V_\theta^0(r,z)$ is defined by

$$V_\theta^0(r,z) = (\int d^3p v_\theta f_b^0)/(\int d^3p f_b^0) \approx [(P_0/r) + (e/c)A_\theta^0(r,z)]/[\gamma_\theta(r,z)m] . \tag{18}$$

For future reference, we define the characteristic azimuthal energy $\gamma_b mc^2$ of a beam electron by

$$\gamma_b mc^2 \equiv \gamma_\theta(R_0,0)mc^2 , \tag{19}$$

and choose

$$P_0 = \frac{e\hat{B}_z}{2c} R_0^2 , \qquad A_\theta^0(R_0,0) = \frac{1}{2}\hat{B}_z R_0 , \tag{20}$$

where $\hat{B}_z \equiv B_{0z}^{ext}(R_0,0)$.

The mean equilibrium radius R_0 of the ring is effectively determined from the condition[8,9]

$$\left[mc^2 \frac{\partial}{\partial r} \gamma_\theta(r,z) - e \frac{\partial}{\partial r} \phi_0(r,z)\right]_{(R_0,0)} = 0. \tag{21}$$

Making use of Eqs. (16) and (21), we obtain[8,9]

$$\gamma_b m \beta_b^2 c^2 / R_0 = e[E_r^0(R_0,0) + \beta_b B_z^0(R_0,0)] , \tag{22}$$

where $\beta_b \equiv V_\theta^0(R_0,0)/c$, $E_r^0(r,z) = -\partial\phi_0/\partial r$ is the radial self electric field and $B_z^0(r,z) = (1/r)(\partial/\partial r)(rA_\theta^0)$ is the axial magnetic field. Equation (22) is simply a statement of radial force balance on an electron fluid element at $(r,z) = (R_0,0)$. Due to the symmetry of the equilibrium configuration (Fig. 1), it is clear that at the midplane $(z = 0)$, the axial electric field and the radial magnetic field are identically zero. We therefore note that

$$\left(\frac{\partial}{\partial z} \gamma_\theta(r,z)\right)_{(R_0,0)} = 0 = \left(\frac{\partial}{\partial z} \phi_0(r,z)\right)_{(R_0,0)} \tag{23}$$

$$\left(\frac{\partial^2}{\partial r \partial z} \gamma_\theta(r,z)\right)_{(R_0,0)} = 0 = \left(\frac{\partial^2}{\partial r \partial z} \phi_0(r,z)\right)_{(R_0,0)} . \tag{24}$$

Making use of Eqs. (20) - (24), the expression for the total energy H in Eq. (17) can be further simplified by Taylor expanding the expressions for $\gamma_\theta(r,z)$, $\phi_0(r,z)$, etc., about $(r,z) = (R_0,0)$. Introducing the radial betatron frequency ω_r defined by

$$\omega_r^2 = \frac{1}{\gamma_b m}\left(\frac{\partial^2}{\partial r^2}(\gamma_\theta mc^2 - e\phi_0)\right)_{(R_0,0)} , \tag{25}$$

and the axial betatron frequency ω_z,

$$\omega_z^2 = \frac{1}{\gamma_b m}\left(\frac{\partial^2}{\partial z^2}(\gamma_\theta mc^2 - e\phi_0)\right)_{(R_0,0)} , \tag{26}$$

we Taylor expand Eq. (17) about $(r,z) = (R_0,0)$ for a thin ring, retaining terms to quadratic order in $r' = r - R_0$ and z. This gives[7-10]

$$H = \gamma_b mc^2 + \frac{p_r^2 + p_z^2}{2\gamma_b m} + \omega_{cz}\left(1 - \frac{r'}{R_0}\right)\delta P_\theta + \frac{(\delta P_\theta)^2}{2\gamma_b^3 m R_0^2} + \frac{1}{2}\gamma_b m(\omega_r^2 r'^2 + \omega_z^2 z^2) , \tag{27}$$

where ω_{cz} is the relativistic electron cyclotron frequency in the axial magnetic field

$$\omega_{cz} = \frac{e\hat{B}_z}{\gamma_b mc} , \tag{28}$$

and $\hat{B}_z \equiv B_{0z}^{ext}(R_0,0)$. Making use of Eqs. (16), (25), and (26), and the expressions for the equilibrium potentials given in Eqs. (A.6) and (A.9), we find that ω_r^2 and ω_z^2 can be expressed as

$$\omega_r^2 = \omega_{cz}^2(1 - n) + \omega_{pb}^2 \frac{b}{a+b}[\beta_b^2 - (1-f)] , \tag{29}$$

and

$$\omega_z^2 = \omega_{cz}^2 n + \omega_{pb}^2 \frac{a}{a+b}[\beta_b^2 - (1-f)] , \tag{30}$$

where $\beta_b = V_\theta^0(R_0,0)/c$, $\omega_{pb}^2 = 4\pi\hat{n}_b e^2/\gamma_b m$ is the relativistic plasma frequency-squared, $\hat{n}_b = n_b^0(R_0,0)$ is the beam density at $(r,z) = (R_0,0)$, and

$$n = -\left(\frac{r}{B_{0z}^{ext}(r,z)}\frac{\partial}{\partial r}B_{0z}^{ext}(r,z)\right)_{(R_0,0)} , \tag{31}$$

is the external field index.

In the remainder of this article, the equilibrium and stability analysis is restricted to circumstances where the characteristic spread Δ in canonical angular momentum P_θ is sufficiently small that

$$\Delta << \gamma_b m\omega_r a^2 \frac{\omega_r}{\omega_{cz}} \ , \quad \gamma_b^2 m\omega_r a R_0 \ . \tag{32}$$

Within the context of Eq. (32), the δP_θ contributions in Eq. (27) are negligibly small in comparison with the final term, and the total energy H can be approximated by

$$H = \gamma_b mc^2 + \frac{p_r^2 + p_z^2}{2\gamma_b m} + \frac{1}{2}\gamma_b m(\omega_r^2 r'^2 + \omega_z^2 z^2) \ . \tag{33}$$

Referring to Eqs. (12), (13), and (33), and making use of the toroidal polar coordinate system (ρ,ϕ,θ) defined in Eq. (2) and Fig. 1, the combination $H - \omega_b P_\phi$ can then be expressed as

$$H - \omega_b P_\phi = \gamma_b mc^2 + \frac{p_\perp^2}{2\gamma_b m} + \psi(r',z) \ , \tag{34}$$

where $p_\perp^2 \equiv p_\rho^2 + (p_\phi - \gamma_b m\omega_b \rho)^2$ is the transverse momentum-squared in a frame of reference rotating with angular velocity ω_b = const. about the toroidal axis, the envelope function $\psi(r',z)$ is defined by

$$\psi(r',z) = \frac{1}{2}\gamma_b m(\Omega_r^2 r'^2 + \Omega_z^2 z^2) \ , \tag{35}$$

where $r' = r - R_0$, and $\hat{\Omega}_r^2$ and $\hat{\Omega}_z^2$ are defined by

$$\begin{aligned} \hat{\Omega}_r^2 &= \omega_b\omega_{c\theta} - \omega_b^2 + \omega_r^2 \ , \\ \hat{\Omega}_z^2 &= \omega_b\omega_{c\theta} - \omega_b^2 + \omega_z^2 \ , \end{aligned} \tag{36}$$

where ω_r^2 and ω_z^2 are defined in Eqs. (29) and (30), and

$$\omega_{c\theta} = \frac{e\hat{B}_\theta}{\gamma_b mc} \ , \tag{37}$$

is the relativistic cyclotron frequency in the applied toroidal magnetic

field $\hat{B}_\theta = B_{0\theta}^{ext}(R_0,0)$. Substituting Eqs. (34) and (35) into Eq. (13) and evaluating the electron density profile $n_b^0(r,z) = \int d^3p f_b^0$, we find

$$n_b^0(r,z) = \hat{n}_b U\left[1 - \left(\frac{r'^2}{a^2} + \frac{z^2}{b^2}\right)\right] , \tag{38}$$

where $a = [2(\hat{\gamma} - \gamma_b)c^2/\gamma_b\hat{\Omega}_r^2]^{1/2}$ and $b = [2(\hat{\gamma} - \gamma_b)c^2/\gamma_b\hat{\Omega}_z^2]^{1/2}$, and U(x) is the Heaviside step function defined by

$$U(x) = \begin{cases} 1 , & x > 0 , \\ 0 , & x < 0 . \end{cases}$$

Note from Eq. (38) that the electron density is constant ($\hat{n}_b$) inside the beam cross section $r'^2/a^2 + z^2/b^2 \leq 1$, and identically zero outside.

As indicated earlier in this section and in Appendix A, P_ϕ is a good invariant (strictly speaking) provided Eq. (8) is satisfied and provided the beam is circular with a = b and n = 1/2. From Eqs. (29), (30), and (36), we therefore find $\omega_r^2 = \omega_z^2 = \omega_\beta^2$ and $\hat{\Omega}_r^2 = \hat{\Omega}_z^2 = \Omega_\beta^2$ where

$$\omega_\beta^2 \equiv \frac{1}{2}\omega_{cz}^2 + \frac{1}{2}\omega_{pb}^2[\beta_b^2 - (1-f)] , \tag{39}$$

and

$$\Omega_\beta^2 \equiv \omega_b\omega_{c\theta} - \omega_b^2 + \omega_\beta^2 . \tag{40}$$

Moreover, the minor radius of the ring is given by

$$a = b = [2(\hat{\gamma} - \gamma_b)c^2/\gamma_b\Omega_\beta^2]^{1/2} . \tag{41}$$

For existence of the equilibrium, both $\hat{\gamma} > \gamma_b$ and $\Omega_\beta^2 > 0$ are required. The condition $\Omega_\beta^2 > 0$ can be expressed in the equivalent form [Eqs. (39) and (40)]

$$\omega_b^- < \omega_b < \omega_b^+ , \tag{42}$$

where the frequencies $\omega_b^{\pm}$ are defined by

$$\omega_b^{\pm} \equiv \frac{\omega_{c\theta}}{2}\left\{1 \pm \left[1 + \frac{2\omega_{cz}^2}{\omega_{c\theta}^2} - \frac{2\omega_{pb}^2}{\omega_{c\theta}^2}(1-f-\beta_b^2)\right]^{1/2}\right\}. \tag{43}$$

The requirement that the radical in Eq. (43) be real determines the maximum allowable equilibrium beam density for given values of f, β_b^2, ω_{cz}, and $\omega_{c\theta}$. For example, if f = 0, then

$$\frac{2\omega_{pb}^2}{\gamma_b^2} < 2\omega_{cz}^2 + \omega_{c\theta}^2 , \tag{44}$$

is required for existence of the equilibrium. For $\omega_{c\theta}^2 >> \omega_{cz}^2$, Eq. (44) is identical to the result obtained by Sprangle and Kapetanakos[1] within the context of a model that examines the stability of single-particle orbits.

Finally, we conclude this section by noting that Eqs. (13), (32), (34), and (35) can be used to evaluate a variety of equilibrium properties[8,9] for a circular beam with a = b and n = 1/2. For example, the mean rotational velocity $V_\phi^0 = (\int d^3p v_\phi f_b^0)/(\int d^3p f_b^0)$ of an electron fluid element about the toroidal axis is given by

$$V_\phi^0 = \omega_b \rho , \tag{45}$$

where the rotation frequency ω_b is restricted to the range in Eq. (42). Moreover, it can be shown that the equilibrium pressure tensor in the (ρ,ϕ) plane perpendicular to the θ-direction is isotropic with the perpendicular pressure $P_\perp^0(\rho) = n_b^0(\rho)T_\perp^0(\rho)$ given by

$$n_b^0(\rho)T_\perp^0(\rho) = 2\pi \int_0^\infty dp_\perp p_\perp \int_{-\infty}^{\infty} dp_\theta \frac{p_\rho^2 + (p_\phi - \gamma_b m\rho\omega_b)^2}{2\gamma_b m} f_b^0 , \tag{46}$$

where $T_\perp^0(\rho)$ is the effective transverse temperature profile. Defining

$$\hat{T}_\perp \equiv \frac{1}{2}\gamma_b m\Omega_\beta^2 a^2 = \frac{1}{2}\gamma_b m\omega_{c\theta}^2 r_L^2 , \tag{47}$$

and substituting Eq. (13) into Eq. (46) gives

$$T_\perp^0(p) = \hat{T}_\perp(1 - \rho^2/a^2) , \tag{48}$$

for $0 < \rho < a$. In Eq. (47), r_L is the characteristic thermal Larmor radius of the ring electrons in the azimuthal magnetic field $\hat{B}_\theta$. Making use of Eq. (47) to eliminate Ω_β in Eq. (40) in favor of r_L, we solve Eq. (40) for the rotation frequency ω_b and obtain

$$\omega_b = \hat{\omega}_b^{\pm} \equiv \frac{\omega_{c\theta}}{2}\left\{1 \pm \left[1 + \frac{2\omega_{cz}^2}{\omega_{c\theta}^2} - \frac{2\omega_{pb}^2}{\omega_{c\theta}^2}(1 - f - \beta_b^2) - \left(\frac{2r_L}{a}\right)^2\right]^{1/2}\right\}, \tag{49}$$

which relates ω_b to the Larmor radius r_L. The two signs (±) in Eq. (49) represent fast (+) and slow (-) rotational equilibria. In order for the equilibrium to exist, the ratio $2r_L/a$ in Eq. (49) is restricted to the range

$$\left(\frac{2r_L}{a}\right)^2 \leq 1 - \frac{2\omega_{pb}^2}{\omega_{c\theta}^2}(1 - f - \beta_b^2) + \frac{2\omega_{cz}^2}{\omega_{c\theta}^2} . \tag{50}$$

LINEARIZED VLASOV-MAXWELL EQUATIONS

In this section, we make use of the linearized Vlasov-Maxwell equations to investigate stability properties of the equilibrium ring configuration discussed in Sec. II. In the stability analysis, a normal-mode approach is adopted in which all perturbed quantities are assumed to vary according to

$$\delta\psi(\underset{\sim}{x},t) = \delta\hat{\psi}(\underset{\sim}{x})\exp(-i\omega t)$$
$$= \delta\hat{\psi}(\rho)\exp[i(\ell\theta - \omega t)] ,$$

where $\mathrm{Im}\omega > 0$, $\rho \equiv [(r - R_0)^2 + z^2]^{1/2}$, and $\partial/\partial\Phi = 0$ is assumed (Fig. 1). Here, ω is the complex oscillation frequency and ℓ is the toroidal harmonic number. Integrating from $t' = -\infty$ to $t' = t$ and neglecting initial perturbations, we find that the perturbed distribution function can be expressed as $\delta f_b(\underset{\sim}{x},\underset{\sim}{p},t) = \delta\hat{f}_b(\underset{\sim}{x},\underset{\sim}{p})\exp(-i\omega t)$, where

$$\delta\hat{f}_b(\underset{\sim}{x},\underset{\sim}{p}) = e\int_{-\infty}^{0} d\tau\, \exp(-i\omega\tau)$$
$$\times \left\{\delta\hat{\underset{\sim}{E}}(\underset{\sim}{x}') + \frac{1}{c}\,\underset{\sim}{v}' \times \delta\hat{\underset{\sim}{B}}(\underset{\sim}{x}')\right\} \cdot \frac{\partial}{\partial \underset{\sim}{p}'}\, f_b^0(\underset{\sim}{x}',\underset{\sim}{p}'). \tag{51}$$

In Eq. (51), $\tau = t' - t$, $\delta\hat{\underset{\sim}{E}}(\underset{\sim}{x})$ and $\delta\hat{\underset{\sim}{B}}(\underset{\sim}{x})$ are the perturbed electromagnetic field amplitudes, and the particle trajectories $\underset{\sim}{x}'(t')$ and $\underset{\sim}{v}'(t')$ satisfy $d\underset{\sim}{x}'/dt' = \underset{\sim}{v}'$ and $d\underset{\sim}{p}'/dt' = -e[\underset{\sim}{E}^0 + \underset{\sim}{v}' \times \underset{\sim}{B}^0/c]$ with "initial" conditions $\underset{\sim}{x}'(t' = t) = \underset{\sim}{x}$ and $\underset{\sim}{v}'(t' = t) = \underset{\sim}{v}$. The Maxwell equations for $\delta\hat{\underset{\sim}{E}}(\underset{\sim}{x})$ and $\delta\hat{\underset{\sim}{B}}(\underset{\sim}{x})$ are given by

$$\nabla \times \delta\hat{\underset{\sim}{E}} = \frac{i\omega}{c}\,\delta\hat{\underset{\sim}{B}} , \tag{52}$$

$$\nabla \times \delta\hat{\underset{\sim}{B}} = \frac{4\pi}{c}\,\delta\hat{\underset{\sim}{J}} - \frac{i\omega}{c}\,\delta\hat{\underset{\sim}{E}} , \tag{53}$$

where $\nabla \cdot \delta\hat{\underset{\sim}{B}} = 0$ and

$$\nabla \cdot \delta\hat{\underset{\sim}{E}} = 4\pi\delta\hat{\rho} \ . \tag{54}$$

In Eqs. (53) and (54) the perturbed current and charge densities are defined by

$$\delta\hat{\underset{\sim}{J}}(\underset{\sim}{x}) = -e\int d^3p \ \underset{\sim}{v} \ \delta\hat{f}_b \ , \tag{55}$$

$$\delta\hat{\rho}(\underset{\sim}{x}) = -e\int d^3p \ \delta\hat{f}_b \ , \tag{56}$$

where $\underset{\sim}{v} = \underset{\sim}{p}/\gamma m$. Taking the curl of Eq. (52) and making use of Eqs. (53) and (54), we obtain

$$\left(\nabla^2 + \frac{\omega^2}{c^2}\right)\delta\hat{\underset{\sim}{E}} = 4\pi\left(\nabla\delta\hat{\rho} - \frac{i\omega}{c^2}\,\delta\hat{\underset{\sim}{J}}\right) , \tag{57}$$

which is the form of Maxwell's equations used in the present stability analysis.

For present purposes, we consider $\partial/\partial\Phi = 0$ wave perturbations with polarization

$$\begin{aligned} \delta\hat{\underset{\sim}{E}}\,(\underset{\sim}{x}) &= \delta\hat{E}_\theta(\rho,\theta)\hat{\underset{\sim}{e}}_\theta + \delta\hat{E}_\rho(\rho,\theta)\hat{\underset{\sim}{e}}_\rho \\ &= \exp\,(i\ell\theta)[\delta\hat{E}_\theta(\rho)\hat{\underset{\sim}{e}}_\theta + \delta\hat{E}_\rho(\rho)\hat{\underset{\sim}{e}}_\rho] \ , \\ \delta\hat{\underset{\sim}{B}}\,(\underset{\sim}{x}) &= \delta\hat{B}_\Phi(\rho,\theta)\hat{\underset{\sim}{e}}_\Phi = \exp\,(i\ell\theta)\delta\hat{B}_\Phi(\rho)\hat{\underset{\sim}{e}}_\Phi , \end{aligned} \tag{58}$$

where $\hat{\underset{\sim}{e}}_\theta$, $\hat{\underset{\sim}{e}}_\rho$ and $\hat{\underset{\sim}{e}}_\Phi$ are unit vectors in the θ-,ρ- and Φ-directions, respectively (Fig. 1). Approximating $i\ell/r \simeq i\ell/R_0 = ik$, it is straightforward to show from the Φ-component of Eq. (52) and the ρ-component of Eq. (53) that $\delta B_\Phi(\rho)$ can be expressed as

$$\begin{aligned} \delta B_\Phi(\rho) &= \frac{ic}{\omega}\frac{\partial}{\partial\rho}\,\delta\hat{E}_\theta(\rho) + \frac{kc}{\omega}\delta\hat{E}_\rho(\rho) \ , \\ &= \frac{1}{\omega^2/c^2k^2 - 1}\left[\frac{\omega^2}{c^2k^2}\frac{ic}{\omega}\frac{\partial}{\partial\rho}\,\delta\hat{E}_\theta(\rho) - \frac{4\pi i}{ck}\delta\hat{J}_\rho(\rho)\right] , \end{aligned} \tag{59}$$

where the perturbed current $\delta\hat{J}_\rho$ is related to $\delta\hat{B}_\phi$ and $\delta\hat{E}_\rho$ by $-ik\delta\hat{B}_\phi = (4\pi/c)\delta\hat{J}_\rho - (i\omega/c)\delta\hat{E}_\rho$. We also assume that the toroidal conductor (radius $\rho = a_c$) has large aspect ratio with

$$a_c << R_0. \tag{60}$$

Taking the θ-component of Eq. (57), we obtain the eigenvalue equation for $\delta\hat{E}_\theta$,

$$\left[\frac{1}{\rho}\frac{\partial}{\partial\rho}\rho\frac{\partial}{\partial\rho} + \left(\frac{\omega^2}{c^2} - k^2\right)\right]\delta\hat{E}_\theta = 4\pi\left(ik\delta\hat{\rho} - \frac{i\omega}{c^2}\delta\hat{J}_\theta\right), \tag{61}$$

where $k = \ell/R_0$, and we have approximated $\nabla^2 = \nabla_\perp^2 - \ell^2/r^2 \simeq \rho^{-1}(\partial/\partial\rho) \times (\rho\partial/\partial\rho) - k^2$ in Eq. (61). It is further assumed that $\mathrm{Re}\omega = \Omega_r$ satisfies $\Omega_r \tilde{\simeq} \ell\omega_{cz}$, and that the waves are far removed from resonance with the transverse (r,z) motion, with[10]

$$\left|\left(\frac{\omega_b^\pm}{\omega - \ell\omega_{cz}}\right)^2 - 1\right|, \quad \left|\frac{\omega_b^\pm}{\omega}\right| >> \frac{a}{R_0}, \tag{62}$$

where $\omega_b^\pm$ are the characteristic (r',z') orbit oscillation frequencies about $(r,z) = (R_0,0)$ [Eq. (43) and Appendix B]. To lowest order, consistent with Eq. (62), it is shown in Appendix B that the azimuthal orbit is described by [Eq. (B.14)]

$$\theta' = \theta + (\omega_{cz} - \mu\delta P_\theta/\gamma_b m R_0^2)\tau, \tag{63}$$

where $\tau = t' - t$,

$$\mu = \frac{\omega_{cz}^2}{\omega_\beta^2} - \frac{1}{\gamma_b^2}, \tag{64}$$

and $\omega_\beta^2 = \omega_{cz}^2/2 + (\omega_{pb}^2/2)[\beta_b^2 - (1-f)]$ for a circular beam with a = b and n = 1/2.

From Eqs. (51), (58), and (59), we note that

$$\delta\hat{\underset{\sim}{E}}(\underset{\sim}{x}') + \frac{\underset{\sim}{v}' \times \delta\hat{\underset{\sim}{B}}(\underset{\sim}{x}')}{c}$$

$$= \exp(i\ell\theta')\left[\delta\hat{E}_\theta(\rho') + \frac{v_\rho'}{c}\left(\frac{ic}{\omega}\frac{\delta}{\delta\rho'}\delta\hat{E}_\theta(\rho') + \frac{kc}{\omega}\delta\hat{E}_\rho(\rho')\right)\right]\hat{\underset{\sim}{e}}_\theta \qquad (65)$$

$$+ \exp(i\ell\theta')\left[\delta\hat{E}_\rho(\rho') - \frac{v_\theta'}{c}\left(\frac{ic}{\omega}\frac{\partial}{\partial\rho'}\delta\hat{E}_\theta(\rho') + \frac{kc}{\omega}\delta\hat{E}_\rho(\rho')\right)\right]\hat{\underset{\sim}{e}}_\rho .$$

Estimating the size of terms proportional to $\delta\hat{E}_\rho$ and $\partial\delta\hat{E}_\theta/\partial\rho'$ in Eq. (65), and making use of the assumption that the wave perturbations are far removed from resonance with the transverse (r', z') motion [Eq. (62) and Appendix B], it is straightforward to show that the terms proportional to $\partial\delta\hat{E}_\theta/\partial\rho'$ and $\delta\hat{E}_\rho$ in Eq. (65) can be neglected in comparison with $\delta\hat{E}_\theta\hat{\underset{\sim}{e}}_\theta$. Moreover, making use of $\partial f_b^0(H, P_\phi, P_\theta)/\partial p_\theta = v_\theta \partial f_b^0/\partial H + r\partial f_b^0/\partial P_\theta$, we find that $\delta\hat{f}_b(\underset{\sim}{x}, \underset{\sim}{p})$ in Eq. (51) can be approximated by

$$\delta\hat{f}_b(\underset{\sim}{x},\underset{\sim}{p}) = e\frac{\partial f_b^0}{\partial P_\theta}\exp(i\ell\theta)\int_{-\infty}^{0} d\tau(R_0 + \rho'\cos\phi')\delta\hat{E}_\theta(\rho')\exp[i\ell(\theta' - \theta) - i\omega\tau]$$

$$+ e\frac{\partial f_b^0}{\partial H}\exp(i\ell\theta)\int_{-\infty}^{0} d\tau v_\theta'\delta\hat{E}_\theta(\rho')\exp[i\ell(\theta' - \theta) - i\omega\tau], \qquad (66)$$

where $\theta'(\tau)$ is defined in Eq. (63), and use has been made of the fact that $\partial f_b^0/\partial P_\theta$ and $\partial f_b^0/\partial H$ are independent of t'. In Eq. (66), it follows from Eq. (63) that $v_\theta' = (R_0 + \rho'\cos\phi')(\omega_{cz} - \mu\delta P_\theta/\gamma_b m R_0^2)$. To simplify Eq. (66), we approximate $R_0 + \rho'\cos\phi' \simeq R_0$ to lowest order, and Taylor expand $\delta\hat{E}_\theta(\rho') = \delta\hat{E}_\theta(\rho) + [\partial\delta\hat{E}_\theta(\rho)/\partial\rho](\rho' - \rho) + \ldots$ locally about $\rho' = \rho$. For present purposes, we also approximate $\delta\hat{E}_\theta(\rho') \simeq \delta\hat{E}_\theta(\rho)$, which is a good approximation provided $r_L << a$ [Eqs. (49) and (50)]. Carrying out the t' integration in Eq. (66) then gives

$$\delta\hat{f}_b(\underset{\sim}{x},\underset{\sim}{p}) = ie\exp(i\underset{\sim}{k}\cdot\underset{\sim}{x})\hat{E}_\theta(\rho)R_0 \times \frac{\left(\frac{\partial f_b^0}{\partial P_\theta} + (\omega_{cz} - \mu\delta P_\theta/\gamma_b mR_0^2)\frac{\partial f_b^0}{\partial H}\right)}{(\omega - \ell\omega_{cz} + \ell\mu\delta P_\theta/\gamma_b mR_0^2)} \quad (67)$$

To complete the description, we evaluate $4\pi(ik\delta\hat{\rho} - i\omega\delta\hat{J}_\theta/c^2) = -4\pi ei k\int d^3p\delta\hat{f}_b(1 - \omega p_\theta/c^2 k\gamma m)$ on the right-hand side of Eq. (61). To the required accuracy, $(1 - \omega P_\theta/c^2 k\gamma m)$ can be approximated in the integrand by $(1 - \omega\beta_b/ck) - \omega\delta P_\theta/c^2 k\gamma_b mR_0$, where $\omega \simeq \ell\omega_{cz} = k\omega_{cz}R_0 = k\beta_b c$ is assumed. Making use of Eqs. (56), (61) and (67) then gives the eigenvalue equation

$$\left[\frac{1}{\rho}\frac{\partial}{\partial\rho}\rho\frac{\partial}{\partial\rho} + \left(\frac{\omega^2}{c^2} - k^2\right)\right]\delta\hat{E}_\theta(\rho) = 4\pi e^2\ell\delta\hat{E}_\theta(\rho)\int d^3p\left[\left(1 - \beta_b\frac{\omega}{ck}\right) - \frac{\omega}{ck}\frac{\delta P_\theta}{\gamma_b mR_0 c}\right] \times \frac{\left[\frac{\partial f_b^0}{\partial P_\theta} + \left(\omega_{cz} - \mu\frac{\delta P_\theta}{\gamma_b mR_0^2}\right)\frac{\partial f_b^0}{\partial H}\right]}{\omega - \ell\omega_{cz} + \ell\mu\delta P_\theta/\gamma_b mR_0^2} \quad (68)$$

Paralleling the analysis in Ref. 10, the integral contribution proportional to $\int d^3p \ldots \partial f_b^0/\partial H$ gives <u>surface-charge</u> contributions on the right-hand side of Eq. (68) proportional to $\partial n_b^0(\rho)/\partial\rho = -\hat{n}_b\delta(\rho-a)$ [Eq. (38)]. Although this surface-charge contribution can be retained in a self-consistent manner, for present purposes we neglect the term proportional to $\partial f_b^0/\partial H$ in Eq. (68) and retain only the negative-mass and resistive wall effects associated with $\partial f_b^0/\partial P_\theta$. This is a valid approximation provided the beam density ω_{pb}^2 satisfies Eq. (44). Integrating over $\partial f_b^0/\partial P_\theta$, Eq. (68) then reduces to

$$\left[\frac{1}{\rho}\frac{\partial}{\partial\rho}\,\rho\,\frac{\partial}{\partial\rho}+\left(\frac{\omega^2}{c^2}-k^2\right)\right]\delta\hat{E}_\theta(\rho)=-\frac{\chi_b(\omega)}{a^2}\,U\,(a-\rho)\delta\hat{E}_\theta(\rho)\ , \qquad (69)$$

where the susceptibility $\chi_b(\omega)$ is defined by

$$\chi_b(\omega)=-\frac{\omega_{pb}^2k^2a^2}{(\omega-\ell\omega_{cz}+i|\mu k\Delta|/\gamma_b mR_0)^2}\left[\mu\left(1-\beta_b\frac{\omega}{ck}\right)+\frac{\omega(\omega-\ell\omega_{cz})}{c^2k^2}\right],$$

for the choice of equilibrium distribution function f_b^0 in Eq. (13). Since $\omega=\ell\omega_{cz}=k\beta_b c$ is assumed, the square-bracket factor in the preceding expression for $\chi_b(\omega)$ can be approximated by $\mu(1-\beta_b^2)=\mu/\gamma_b^2$ and the susceptibility reduces to the approximate expression

$$\chi_b(\omega)=-\mu\frac{\omega_{pb}^2k^2a^2/\gamma_b^2}{(\omega-\ell\omega_{cz}+i|\mu k\Delta|/\gamma_b mR_0)^2}\ . \qquad (70)$$

For the choice of f_b^0 in Eq. (13), we note from Eq. (38) that the density profile $n_b^0(\rho)=\hat{n}_b U(a-\rho)$ is constant in the beam interior. Here, $U(a-\rho)=+1$ for $\rho<a$ and $U(a-\rho)=0$ for $\rho>a$, so that the contribution on the right-hand side of Eq. (69) corresponds to a body-charge perturbation.

Of course, the eigenvalue equation (69) must be solved subject to the appropriate boundary conditions. At the beam boundary $\rho=a$, these conditions are that $\delta\hat{E}_\theta(\rho)$ and $\partial\delta\hat{E}_\theta(\rho)/\partial\rho$ be continuous. At the conducting wall ($\rho=a_c>a$), we assume that the wall has finite conductivity σ. The boundary condition at the wall can then be approximated by[11]

$$\delta\hat{E}_\theta(a_c)=-\frac{\omega\delta}{2c}(1-i)\,\delta\hat{B}_\phi(a_c)$$

$$=\frac{\delta}{2}\beta_b^2\gamma_b^2(1+i)\left[\frac{\partial}{\partial\rho}\,\delta\hat{E}_\theta(\rho)\right]_{\rho=a_c}\ . \qquad (71)$$

In obtaining Eq. (71), use has been made of Eq. (59) on the vacuum side (where $\delta\hat{J}_\rho = 0$) of the conducting wall, and we have approximated $(1 - \omega^2/c^2k^2)^{-1} = \beta_b^2\gamma_b^2$ for $\omega \approx \ell\omega_{cz} = k\beta_b c$. In Eq. (71)

$$\delta = c/(2\pi\omega\sigma)^{1/2}, \tag{72}$$

is the skin depth in the wall.

Equation (69) can be further simplified for $|\chi_b| \gtrsim 1$ and $\omega = \ell\omega_{cz} = k\omega_{cz}R_0$. In this case,

$$\left(k^2 - \frac{\omega^2}{c^2}\right) = \frac{\ell^2 a^2}{R_0^2\gamma_b^2} << 1,$$

which is consistent with Eq. (62). Equation (69) can then be approximated by

$$\left(\frac{1}{\rho}\frac{\partial}{\partial\rho}\rho\frac{\partial}{\partial\rho} + T^2\right)\delta\hat{E}_\theta(\rho) = 0, \qquad 0 \le \rho < a, \tag{73}$$

and

$$\frac{1}{\rho}\frac{\partial}{\partial\rho}\rho\frac{\partial}{\partial\rho}\delta\hat{E}_\theta(\rho) = 0, \qquad a < \rho \le a_c, \tag{74}$$

where

$$T^2a^2 = \chi_b(\omega) \tag{75}$$

and $\chi_b(\omega)$ is defined in Eq. (70). The physically acceptable solutions to Eqs. (73) and (74) with $\delta\hat{E}_\theta(\rho)$ and $\partial\delta\hat{E}_\theta/\partial\rho$ continuous at $\rho = a$ are given by

$$\delta\hat{E}_\theta(\rho) = \begin{cases} AJ_0(T\rho), & 0 \le \rho < a \\ AJ_0(Ta)\left(1 + Ta\dfrac{J_0'(Ta)}{J_0(Ta)}\ell n\dfrac{\rho}{a}\right), & a < \rho \le a_c \end{cases} \tag{76}$$

where $J_0(x)$ is the Bessel function of the first kind of order zero, and $J_0'(x) = dJ_0(x)/dx$. Enforcing Eq. (76) at the conducting wall $\rho = a_c$ gives the required dispersion relation

$$J_0(Ta) - J_1(Ta)\left[\ell n\,\frac{a_c}{a} - \frac{1}{2}\,(1+i)\,\frac{\delta}{a_c}\,\beta_b^2\gamma_b^2\right] = 0\ , \qquad (77)$$

where use has been made of $J_1(x) = -xJ_0'(x)$.

Equation (77) is a transcendental equation for the complex eigenfrequency ω and must be solved numerically in the general case. There are two limiting regimes, however, where Eq. (77) can be simplified analytically.

(a) $a_c >> a$ or $\beta_b^2\gamma_b^2\delta >> a_c$: There is a large temptation to Taylor expand Eq. (77) for

$$|T|^2a^2 << 1. \qquad (78)$$

To lowest order this gives the approximate dispersion relation

$$1 - \frac{1}{4}\,T^2a^2\left[\left(1 + 2\ell n\,\frac{a_c}{a}\right) - \frac{\delta}{a_c}\,(1+i)\,\beta_b^2\gamma_b^2\right] = 0\ . \qquad (79)$$

From Eq. (79), it is evident that Eq. (78) is a valid approximation only if

$$\frac{1}{4}\left|\left(1 + 2\ell n\,\frac{a_c}{a}\right) - \frac{\delta}{a_c}\,(1+i)\,\beta_b^2\gamma_b^2\right| >> 1 \qquad (80)$$

is satisfied. Equation (80) typically requires a large conducting wall radius $a_c >> a$, or $\beta_b^2\gamma_b^2\delta >> a_c$ in order for the inequality to be satisfied. Making use of Eqs. (70) and (75), the dispersion relation in Eq. (79) reduces to

$$(\omega - \ell\omega_{cz} + i|\mu k\Delta|/\gamma_b mR_0)^2 = -\frac{1}{4}\,\mu\frac{\omega_{pb}^2k^2a^2}{\gamma_b^2}\left[\left(1 + 2\ell n\,\frac{a_c}{a}\right) - \frac{\delta}{a_c}\,(1+i)\,\beta_b^2\gamma_b^2\right]. \qquad (81)$$

Equation (77) also supports solutions with $|T|^2a^2 \gtrsim 1$ when the inequality in Eq. (80) is satisfied. Making use of Eq. (80), we find that the dispersion relation in Eq. (77) can be approximated by

$$J_1(Ta) = 0 , \tag{82}$$

which gives $T^2a^2 = \lambda_{1n}^2$, $n = 1,2,\ldots$ where $J_1(\lambda_{1n}) = 0$ and λ_{1n} is the n'th zero of $J_1(x) = 0$. Making use of Eqs. (70), (75), and (82), we obtain the dispersion relation

$$(\omega - \ell\omega_{cz} + i|\mu k\Delta|/\gamma_b mR_0)^2 = -\mu\omega_{pb}^2 \frac{k^2a^2/\gamma_b^2}{\lambda_{1n}^2} , \qquad n = 1,2,\ldots \tag{83}$$

where $J_1(\lambda_{1n}) = 0$.

Equation (83) is really an extension of the dispersion relation (81) from the regime $|T|^2a^2 << 1$ to the regime $|T|^2a^2 \gtrsim 1$. What is most important to note is that Eq. (83) is independent of wall resistivity, whereas Eq. (81) is not. Moreover, the characteristic growth rate $\Omega_i = \mathrm{Im}\omega$ obtained from Eq. (81) is larger than that obtained from Eq. (83). Indeed the mode is rapidly stabilized for increasing λ_{1n}^2.

(b) $a_c \approx a$ and $\beta_b^2\gamma_b^2\delta << a_c$. In circumstances where $\beta_b^2\gamma_b^2\delta << a_c$ and the beam radius is approximately equal to the conducting wall radius $a \approx a_c$, the coefficient of $J_1(Ta)$ in Eq. (77) is algebraically small, and the dispersion relation (77) can be approximated by

$$J_0(Ta) = 0 , \tag{84}$$

which has solutions $T^2a^2 = \lambda_{0n}^2$, $n = 1,2,\ldots$, where λ_{0n} is the n'th zero of $J_0(\lambda_{0n}) = 0$. Making use of Eqs. (70), (75), and (84), the dispersion relation (84) gives

$$(\omega - \ell\omega_{cz} + i|\mu k\Delta|/\gamma_b mR_0)^2$$

$$\approx -\mu\omega_{pb}^2 \frac{k^2 a^2}{\gamma_b^2 \lambda_{0n}^2}, \quad n = 1,2 \ldots \tag{85}$$

where $J_0(\lambda_{0n}) = 0$. The most unstable solution associated with Eq. (85) is the fundamental mode with $n = 1$. As in Eq. (83), the growth rate $\mathrm{Im}\omega$ decreases rapidly for increasing λ_{0n}^2. Comparing Eqs. (81) and (85), we note that placing the conducting wall radius (a_c) near the beam radius (a) significantly reduces the growth rate.

NEGATIVE-MASS INSTABILITY

We now make use of the dispersion relations (81) and (85) derived in Sec. III to determine negative-mass stability properties for the case where the wall is perfectly conducting with $\delta = 0$. Introducing the geometric factor

$$g = \begin{cases} \left(1 + 2\ell n \dfrac{a_c}{a}\right) , & \text{for } a_c >> a , \\ \dfrac{4}{\lambda_{0n}^2} , & \text{for } a_c = a , \end{cases} \tag{86}$$

and approximating $k^2 - \omega^2/c^2 = k^2(1 - \omega_{cz}^2 R_0^2/c^2) = k^2/\gamma_b^2$ for $\omega = \ell\omega_{cz}$, the dispersion relations (81) and (85) can be expressed as

$$(\omega - \ell\omega_{cz} + i|\mu k\Delta|/\gamma_b mR_0)^2 = -\mu\omega_{pb}^2 \frac{k^2a^2}{\gamma_b^2}\frac{g}{4} . \tag{87}$$

Solving Eq. (87) for ω, we find that the necessary and sufficient condition for instability ($\mathrm{Im}\omega > 0$) is that

$$0 < \mu < \frac{\nu}{\gamma_b}\left(\frac{mR_0c}{\Delta}\right)^2 g, \tag{88}$$

where $\nu = (\hat{n}_b \pi a^2)(e^2/mc^2)$ is Budker's parameter for the beam, and g is defined in Eq. (86). When the inequalities in Eq. (88) are satisfied, the real frequency $\Omega_r = \mathrm{Re}\omega$ and growth rate $\Omega_i = \mathrm{Im}\omega$ are given by

$$\Omega_r = \ell\omega_{cz} ,$$
$$\Omega_i = \frac{\ell c}{\gamma_b R_0}\left[\left(\frac{\mu g \nu}{\gamma_b}\right)^{1/2} - \frac{\mu\Delta}{mR_0c}\right] , \tag{89}$$

where $k = \ell/R_0$.

The stability results in Eqs. (87) - (89) can be investigated in various regimes of experimental interest. It is interesting to note from Eq. (87) that a sufficient condition for stability ($Im\omega < 0$) is

$$\mu = \frac{\omega_{cz}^2}{\omega_\beta^2} - \frac{1}{\gamma_b^2} < 0 \ , \tag{90}$$

where $\omega_\beta^2 = \omega_{cz}^2/2 + (\omega_{pb}^2/2)[\beta_b^2 - (1-f)]$. For $f = 0$, the condition $\mu < 0$ [Eq. (90)] and condition for existence of confined equilibria [Eq. (44)] can be expressed as

$$1 < \frac{\omega_{pb}^2}{\gamma_b^2\omega_{cz}^2} < 1 + \frac{\omega_{c\theta}^2}{2\omega_{cz}^2} \ . \tag{91}$$

Evidently, for $f = 0$, the inequality in Eq. (91) can be satisfied provided $\omega_{pb}^2/\omega_{cz}^2$ is sufficiently large. That is, the negative-mass instability can be completely stabilized for $\Delta = 0$ provided equilibrium self-field effects are sufficiently strong.

The regime where $\mu > 0$ is perhaps of more practical interest. In this case, making use of Eqs. (87) and (88), the instability is completely stabilized whenever the inequality

$$\left(\frac{\Delta}{\gamma_b m\beta_b cR_0}\right)^2 > \frac{\nu}{\gamma_b}\left(\frac{g}{\mu\gamma_b^2\beta_b^2}\right) \ , \tag{92}$$

is satisfied. It is evident from Eqs. (86) and (92) that the instability is most difficult to stabilize when $a_c >> a$ and the geometric factor g is large. Even in this case, however, only a modest spread Δ in canonical angular momentum is required for stabilization. As a numerical example, consider the case where $\omega_{pb}^2/\omega_{cz}^2 << 1$ and $\mu \simeq 1 - 1/\gamma_b^2 = \beta_b^2$. For $\nu/\gamma_b = 1/20$, $g = 5$, $\gamma_b = 5$, and $\beta_b = 1$, Eq. (92) predicts stability for $(\Delta/\gamma_b m\beta_b cR_0) > 1/10$.

RESISTIVE WALL INSTABILITY

In this section, we consider the dispersion relation (77) and its limiting versions [e.g., Eq. (81)] in circumstances where wall resistivity effects (as measured by δ/a_c) play an important role. In this regard, since a spread Δ in canonical angular momentum has a stabilizing influence, we first consider the most unstable case with

$$\Delta = 0 , \tag{93}$$

and

$$T^2a^2 = - \frac{\mu}{\gamma_b^2} \frac{\omega_{pb}^2 k^2 a^2}{(\omega - \ell\omega_{cz})^2} . \tag{94}$$

We further consider circumstances where

$$\mu < 0 , \tag{95}$$

and therefore the negative-mass instability is absent (Sec. IV). Assuming <u>weak</u> dissipation in Eq. (77) with $\beta_b^2\gamma_b^2\delta/a_c << 1$, the real oscillation frequency $\Omega_r = \mathrm{Re}\omega$ is determined from

$$J_0(Ta) - J_1(Ta)\left(\ell n \frac{a_c}{a} - \frac{1}{2}\frac{\delta}{a_c}\beta_b^2\gamma_b^2\right) = 0 , \tag{96}$$

and the growth rate $\Omega_i = \mathrm{Im}\omega$ is determined from

$$\Omega_i = \frac{-\frac{1}{2}\frac{\delta}{a_c} J_1(Ta)\beta_b^2\gamma_b^2}{\left[J_0'(Ta) - J_1'(Ta)\left(\ell n \frac{a_c}{a} - \frac{1}{2}\frac{\delta}{a_c}\beta_b^2\gamma_b^2\right)\right]\frac{\partial}{\partial\Omega_r} Ta} \tag{97}$$

where Ta in Eq. (97) solves Eq. (96), and we have neglected the (slow) variation of δ with Ω_r. We now consider Eqs. (77), (96), and (97) in various limiting regimes.

(a) $a_c = a$ and $\Delta = 0$: For $\beta_b^2\gamma_b^2\delta << a_c$, and beam radius equal to the conducting wall radius ($a = a_c$), Eq. (96) reduces approximately to $J_0(Ta) = 0$. Making use of Eqs. (94) and (95), the real frequency Ω_r is given by [Eq. (85)],

$$\Omega_r - \ell\omega_{cz} = \pm|\mu|^{1/2}\frac{\omega_{pb}ka}{\lambda_{0n}\gamma_b}, \quad n = 1,2,\ldots, \tag{98}$$

where $J_0(\lambda_{0n}) = 0$. Moreover, making use of $a_c = a$, $\beta_b^2\gamma_b^2\delta << a_c$ and $xJ_0'(x) = -J_1(x)$, Eq. (97) reduces to

$$\begin{aligned}\Omega_i &= \frac{1}{2}\frac{\delta}{a_c}\frac{Ta}{\partial Ta/\partial\Omega_r}\beta_b^2\gamma_b^2 \\ &= -\frac{1}{2}\frac{\delta}{a_c}(\Omega_r - \ell\omega_{cz})\beta_b^2\gamma_b^2,\end{aligned} \tag{99}$$

and the slow-wave (lower) branch in Eq. (98) corresponds to instability ($\Omega_i > 0$) with growth rate

$$\Omega_i = \frac{1}{2}\frac{\delta}{a_c}\beta_b^2\gamma_b^2|\mu|^{1/2}\frac{\omega_{pb}ka}{\lambda_{0n}\gamma_b}, \quad n = 1,2,\ldots \tag{100}$$

(b) $a_c >> a$ and $\Delta = 0$: For $\beta_b^2\gamma_b^2\delta << a_c$, large conducting wall radius ($a_c >> a$), and $|T|^2a^2 \gtrsim 1$, Eq. (96) reduces approximately to $J_1(Ta) = 0$, and the real oscillation frequency Ω_r is given by [Eq. (83)]

$$(\Omega_r - \ell\omega_{cz}) = \pm|\mu|^{1/2}\frac{\omega_{pb}ka}{\lambda_{1n}\gamma_b}, \tag{101}$$

where $J_1(\lambda_{1n}) = 0$, and use has been made of $\Delta = 0$ and $\mu < 0$. To the accuracy of Eq. (97), we then find

$$\Omega_i = 0, \tag{102}$$

for $|T|^2a^2 \gtrsim 1$.

On the other hand, for $a_c >> a$, the dispersion relation (77) also supports solutions with $|T|^2a^2 << 1$. In this case Eq. (77) reduces to Eqs. (79) and (81), which has solutions (for $\Delta = 0$ and $\beta_b^2\gamma_b^2\delta << a_c$),

$$(\Omega_r - \ell\omega_{cz}) = \pm|\mu|^{1/2}\frac{\omega_{pb}ka}{2\gamma_b}\left(1 + 2\ell n\frac{a_c}{a}\right)^{1/2}, \tag{103}$$

and

$$\Omega_i = -\frac{1}{2}\frac{\delta}{a_c}\beta_b^2\gamma_b^2\frac{(\Omega_r - \ell\omega_{cz})}{\left(1 + 2\ell n\frac{a_c}{a}\right)}. \tag{104}$$

As in Eq. (97), the lower branch in Eq. (102) is unstable with growth rate

$$\Omega_i = \frac{1}{2}\frac{\delta}{a_c}\beta_b^2\gamma_b^2|\mu|^{1/2}\frac{\omega_{pb}ka}{2\gamma_b}\frac{1}{\left(1 + 2\ell n\frac{a_c}{a}\right)^{1/2}}. \tag{105}$$

Comparing Eqs. (100) and (105), it is clear that the resistive-wall instability exhibits the strongest growth when $a_c \approx a$.

(c) $a_c >> a$ and $\Delta \neq 0$: To illustrate the stabilizing influence of a spread Δ in canonical angular momentum on the resistive wall instability, we consider the regime where $|T|^2a^2 << 1$ and make use of Eqs. (79) and (81) to investigate stability properties for $\mu < 0$ and $\Delta \neq 0$. Expanding Eq. (81) for small $\beta_b^2\gamma_b^2\delta/a_c << 1$, we determine $\Omega_r = Re\omega$ and $\Omega_i = Im\omega$ to be given by

$$\Omega_r - \ell\omega_{cz} = -\frac{|\mu|^{1/2}\omega_{pb}ka}{2\gamma_b}\left(1 + 2\ell n\frac{a_c}{a}\right)^{1/2}, \tag{106}$$

$$\Omega_i = \frac{1}{2}\frac{\delta}{a_c}\beta_b^2\gamma_b^2\frac{|\mu|^{1/2}\omega_{pb}ka}{2\gamma_b\left(1 + 2\ell n\frac{a_c}{a}\right)^{1/2}} - \frac{|\mu|k\Delta}{\gamma_b mR_0}, \tag{107}$$

for the unstable branch with $Im\omega = \Omega_i > 0$. From Eq. (107),

we find that the resistive wall instability is completely stabilized by a small spread Δ in canonical angular momentum satisfying

$$\left(\frac{\Delta}{\gamma_b m \beta_b c R_0}\right)^2 > \frac{1}{16}\frac{\delta^2}{a_c^2}\quad\frac{\omega_{pb}^2 a^2 \beta_b^2 \gamma_b^2}{|\mu| c^2\left(1 + 2\ell n \frac{a_c}{a}\right)} . \tag{108}$$

Of course, Eq. (107) reduces to Eq. (105) in the limit $\Delta \to 0$.

CONCLUSIONS

In this paper we have investigated the equilibrium and stability properties of a relativistic electron ring within the framework of the linearized Vlasov-Maxwell equations. The analysis was carried out for perturbations about an electron ring located at the midplane of an externally applied mirror field combined with an applied toroidal field $B_{0\theta}^{ext}$. Equilibrium and stability properties were calculated in Sections II - V for an equilibrium distribution function which incorporates a spread in canonical angular momentum P_θ [Eq. (13)]. Equilibrium properties were calculated in Section II, and one of the most important features of the equilibrium analysis is that the maximum beam density confined in the modified betatron field configuration can be greatly enhanced by the toroidal magnetic field $B_{0\theta}^{ext}$ [Eqs. (43) and (44)]. Moreover, the rotation frequency ω_b in the minor cross section of the ring plays an important role in determining detailed equilibrium properties.

The formal electromagnetic stability analysis was carried out in Section III, and stability properties were calculated for eigenfrequency ω near harmonics of ω_{cz}. A closed dispersion relation [Eq. (77)] was obtained assuming that the electron ring is located inside a toroidal conductor with finite resistivity and minor radius $a_c << R_0$. Negative-mass stability properties were investigated in Section IV for zero resistivity, including the important influence of equilibrium self fields. For a low-density ring, a modest spread Δ in canonical angular momentum stabilizes the negative-mass instability. In a high-density ring with $f = 0$, however, if the self fields are sufficiently strong, the negative-mass instability can be be completely stabilized by equilibrium self-field effects [Eq. (91)].

The stabilizing influence of equilibrium self fields on the negative-mass instability is an important new feature for stable operation of high-current modified betatron accelerators. The resistive-wall instability was examined in Section V. It was shown that resistive-wall instability can also be stabilized by a modest spread Δ in canonical angular momentum

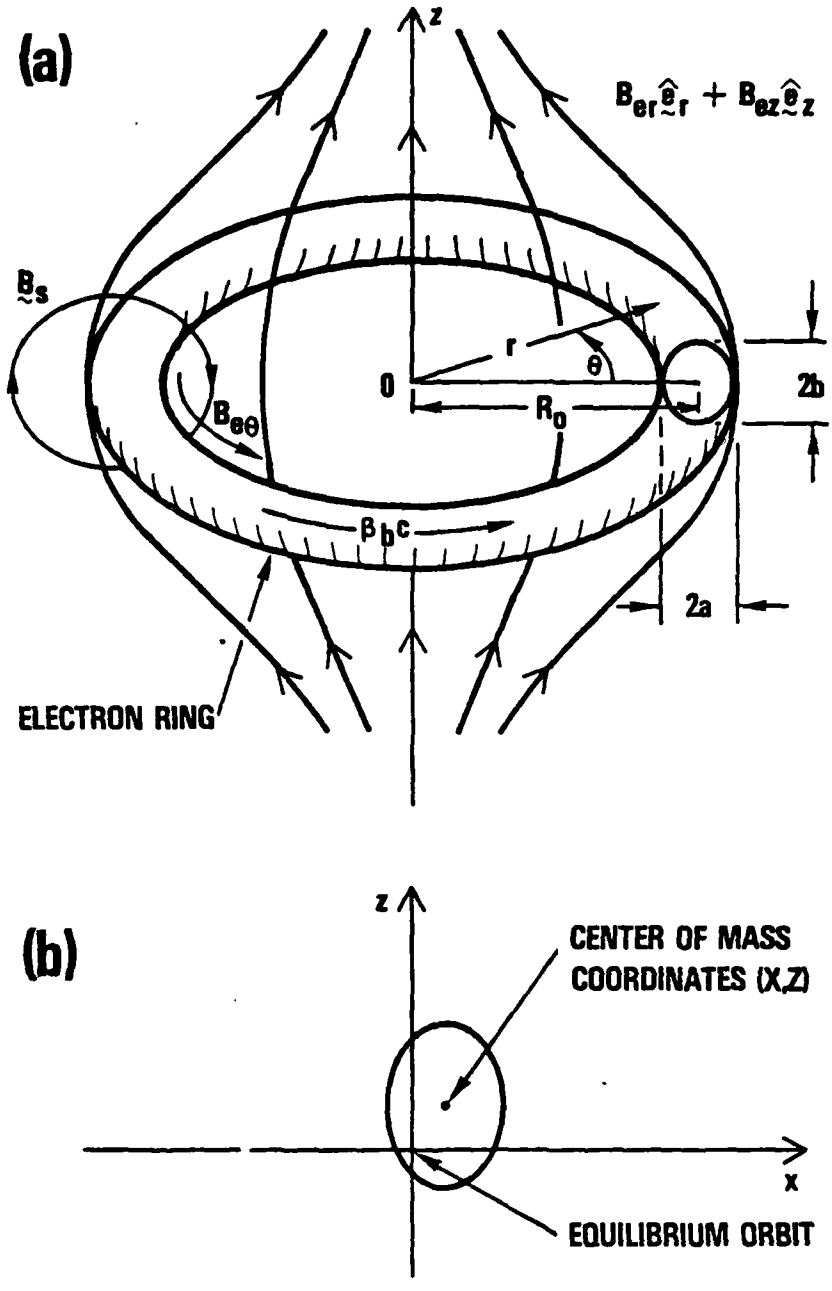

FIGURE 1 EQUILIBRIUM CONFIGURATION AND COORDINATE SYSTEM

ACKNOWLEDGEMENTS

It is a pleasure to acknowledge the benefit of useful discussions with Dr. C. A. Kapetanakos.

This research was supported in part by the Office of Naval Research and in part by the Independent Research fund at the Naval Surface Weapons Center. The research of one of the authors (R.C. Davidson) was supported in part by Office of Naval Research Contract N00014-79-C-0555 with Science Applications, Inc., Boulder, Colorado.

REFERENCES

1. P. Sprangle and C. A. Kapetanakos, J. Appl. Phys. 49, 1 (1978).

2. N. Rostoker, Bull. Am. Phys. Soc. 26, 161 (1980).

3. A. I. Pavlovskii, G. D. Kuleshov, A. I. Gerasimov, A. P. Klementiev, V. O. Kuznetsov, V. A. Tananakin, and A. D. Tarasov, Sov. Phys. Tech. Phys. 22, 218 (1977).

4. A. Fisher, P. Gilad, F. Goldin, and N. Rostoker, Appl. Phys. Lett. 36, 264 (1980).

5. C. E. Nielson, A. M. Sessler, and K. R. Symon in Proceedings of the International Conference on Accelerators (Cern, Geneva, 1959), p. 239.

6. R. W. Landau and V. K. Neil, Phys. Fluids 9, 2412 (1966).

7. R. C. Davidson, H. S. Uhm, and S. M. Mahajan, Phys. Fluids 19, 1608 (1976).

8. R. C. Davidson and J. D. Lawson, Part. Accel. 4, 1 (1972).

9. R. C. Davidson, Theory of Nonneutral Plasmas (Benjamin, Reading, Mass., 1974), pp. 141-154.

10. H. S. Uhm and R. C. Davidson, Phys. Fluids 20, 771 (1977).

11. J. D. Jackson, Classical Electrodynamics (John Wiley & Sons, New York, 1975), Chapter 8.

APPENDIX A

DERIVATION OF APPROXIMATE INVARIANT P_ϕ = CONST. FOR A CIRCULAR BEAM WITH a = b AND n = 1/2

In this Appendix, we make use of the single-particle equations of motion in the equilibrium field configuration and the assumptions outlined in Sec. II to determine the conditions where

$$P_\phi = \rho p_\phi - \frac{1}{2}\frac{e\hat{B}_\theta}{c}\rho^2 , \tag{A.1}$$

is a good approximate invariant. Here, (ρ,ϕ,θ) is the toroidal polar coordinate system defined in Fig. 1 and Eq. (2).

In (r,θ,z) coordinates, the radial and axial equations of motion can be expressed as

$$\dot{p}_r - \frac{v_\theta p_\theta}{r} = F_r = -e\left(E_r^0 + \frac{1}{c}v_\theta B_z^0 - \frac{1}{c}v_z B_\theta^0\right) , \tag{A.2}$$

and

$$\dot{p}_z = F_z = -e\left(E_z^0 + \frac{1}{c}v_r B_\theta^0 - \frac{1}{c}v_\theta B_r^0\right) . \tag{A.3}$$

Here, $E_r^0 = -\partial\phi_0(r,z)/\partial r$ and $E_z^0 = -\partial\phi_0(r,z)/\partial z$ are the radial and axial self electric field components determined from the equilibrium electrostatic potential $\phi_0(r,z)$, and $B_r^0 = B_{0r}^{ext} + B_{0r}^s = -(\partial/\partial z)(A_{0\theta}^{ext} + A_{0\theta}^s)$ and $B_z^0 = B_{0z}^{ext} + B_{0z}^s = r^{-1}(\partial/\partial r)[r(A_{0\theta}^{ext} + A_{0\theta}^s)]$ are the radial and axial components of the total (applied plus self) equilibrium magnetic field. The quantity $A_\theta^0(r,z) = A_{0\theta}^{ext} + A_{0\theta}^s$ is the θ-component of the equilibrium vector potential. Making use of the assumptions enumerated in Eqs. (3), (4), (5), (7), and (9), and considering density and current profiles of the form $n_b^0(r,z) = n_b^0\left(\frac{r'^2}{a^2} + \frac{z^2}{b^2}\right)$ and $J_{\theta b}^0(r,z) = J_{\theta b}^0\left(\frac{r'^2}{a^2} + \frac{z^2}{b^2}\right)$, where $r' = r - R_0$, it is straightforward to

show to the accuracy required in the present analysis that the equilibrium potentials and field components can be approximated in the ring interior ($|r - R_0| = |r'| \lesssim a$ and $|z| \lesssim b$) by[8,9]

$$E_r^0 = -4\pi e(1-f)\hat{n}_b \frac{b}{a+b} r' , \tag{A.4}$$

$$E_z^0 = -4\pi e(1-f)\hat{n}_b \frac{a}{a+b} z , \tag{A.5}$$

$$\phi_0 = \frac{1}{2} 4\pi e(1-f) \frac{\hat{n}_b}{a+b} (br'^2 + az^2) , \tag{A.6}$$

and

$$B_r^0 = -n\hat{B}_z \frac{z}{R_0} - 4\pi eR_0\beta_b\hat{n}_b \frac{a}{a+b} \frac{z}{R_0} , \tag{A.7}$$

$$B_z^0 = \hat{B}_z - n\hat{B}_z \frac{r'}{R_0} + 4\pi eR_0\beta_b\hat{n}_b \frac{b}{a+b} \frac{r'}{R_0} , \tag{A.8}$$

$$\begin{aligned} rA_\theta^0 = {} & R_0A_\theta^0(R_0,0) + R_0\hat{B}_z r' \\ & + \frac{1}{2} (1-n)\hat{B}_z r'^2 + \frac{1}{2} n\hat{B}_z z^2 \\ & + \frac{1}{2} 4\pi eR_0\beta_b \frac{\hat{n}_b}{a+b} (br'^2 + az^2) , \end{aligned} \tag{A.9}$$

where $r' = r - R_0$, $\hat{B}_z \equiv B_{0z}^{ext}(R_0,0)$, $\hat{n}_b \equiv n_b^0(R_0,0)$, $\beta_b \equiv V_\theta^0(R_0,0)/c$, and $n \equiv -[r\partial \ell nB_{0z}^{ext}(r,z)/\partial r]_{(R_0,0)}$ is the external field index. Moreover, from Eq. (1), the applied toroidal field can be approximated by

$$B_\theta^0 = \hat{B}_\theta (1 - r'/R_0) \tag{A.10}$$

in the ring interior.

We make use of Eqs. (A.2) and (A.3) and Eqs. (A.4) - (A.10) to form the difference product

$$z\dot{p}_r - r'\dot{p}_z = \frac{e\hat{B}_\theta}{c}(zv_z + r'v_r)$$

$$+ 4\pi e^2(1 - f)\hat{n}_b \frac{b - a}{a + b} r'z$$

$$- \frac{v_\theta}{c} 4\pi e^2 R_0 \beta_b \hat{n}_b \frac{b - a}{a + b} r'z \qquad (A.11)$$

$$+ zv_\theta \left(\frac{p_\theta}{r} - \frac{e\hat{B}_z}{c} + 2n \frac{e\hat{B}_z}{c} \frac{r'}{R_0}\right) ,$$

where small terms of cubic and higher order ($zr'v_r$, r'^2v_r, etc.) have been neglected in Eq. (A.11). Note that the self-field contributions in Eq. (A.11) vanish identically for a circular beam with a = b. In the final term in Eq. (A.11), we express $p_\theta = P_\theta/r + (e/c)A_\theta^0(r,z) = P_0/r + (e/c)A_\theta^0(r,z) + \delta P_\theta/r$, where $\delta P_\theta = P_\theta - P_0$, and make use of $P_0 = (1/2)(e\hat{B}_z/c)R_0^2$ and $A_\theta^0(R_0,0) = \hat{B}_z R_0/2$. Neglecting terms of cubic order and higher, and assuming a circular beam with a = b, Eq. (A.11) can be approximated by

$$z\dot{p}_r - r'\dot{p}_z = \frac{e\hat{B}_\theta}{c}(zv_z + r'v_r)$$

$$+ v_\theta(2n - 1) \frac{e\hat{B}_z}{c} \frac{r'z}{R_0} \qquad (A.12)$$

$$+ zv_\theta \frac{\delta P_\theta}{R_0^2} .$$

Strictly speaking, a circular beam with a = b requires external field index n = 1/2, so that Eq. (A.12) reduces to

$$z\dot{p}_r - r'\dot{p}_z = \frac{e\hat{B}_\theta}{c}(zv_z + r'v_r) + zv_\theta \frac{\delta P_\theta}{R_0^2} . \qquad (A.13)$$

Comparing the two terms on the right-hand side of Eq. (A.13), and estimating $z \sim r' \sim a$, $v_z \sim v_r \sim p_\perp/\gamma_b m$, and $\gamma_b m v_\theta \sim e\hat{B}_z R_0/c$, we find that the δP_θ contribution in Eq. (A.13) is negligibly small whenever the inequality

$$\frac{|\delta P_\theta|}{\gamma_b m \beta_b c R_0} << \frac{\hat{B}_\theta}{\hat{B}_z}\left|\frac{p_\perp}{p_\theta}\right| , \tag{A.14}$$

is satisfied [Eq. (8)]. Within the context of Eq. (A.14), Eq. (A.13) can be approximated by

$$\frac{d}{dt} P_\phi = \frac{d}{dt}\left(\rho p_\phi - \frac{1}{2}\frac{e\hat{B}_\theta}{c}\rho^2\right) = 0 , \tag{A.15}$$

which is the required result. Here, $\rho^2 = r'^2 + z^2 = (r - R_0)^2 + z^2$, and p_ϕ is the ϕ- component of mechanical momentum in the toroidal polar coordinate system (ρ,ϕ,θ) illustrated in Fig. 1.

APPENDIX B

ELECTRON TRAJECTORIES IN THE EQUILIBRIUM FIELD CONFIGURATION

In this Appendix, we determine the electron orbits in the equilibrium configuration described self-consistently by Eq. (13) in Sec. II and Appendix A. For a circular beam with a = b and n = 1/2, we express the Hamiltonian H in Eq. (27) as

$$H = \gamma_b mc^2 + \frac{1}{2\gamma_b m}\left[\left(P_r' - \frac{1}{2}\gamma_b m\omega_{c\theta} z'\right)^2 + \left(P_z' + \frac{1}{2}\gamma_b m\omega_{c\theta} r'\right)^2\right] + \frac{(\delta P_\theta)^2}{2\gamma_b^3 m R_0^2} + \omega_{cz}(1 - r'/R_0)(\delta P_\theta) + \frac{1}{2}\gamma_b m\omega_\beta^2(r'^2 + z'^2) , \tag{B.1}$$

where (P_r', P_z') are the transverse canonical momenta in the toroidal B_θ^0 field,

$$P_r' = p_r' + \frac{1}{2}\gamma_b m\omega_{c\theta} z' ,$$

$$P_z' = p_z' - \frac{1}{2}\gamma_b m\omega_{c\theta} r' , \tag{B.2}$$

$\omega_\beta^2 = \omega_{cz}^2/2 + (\omega_{pb}^2/2)[\beta_b^2 - (1-f)]$ is the betatron frequency defined in Eq. (39), and $\omega_{c\theta} = e\hat{B}_\theta/\gamma_b mc$ and $\omega_{cz} = e\hat{B}_z/\gamma_b mc$. The "primed" orbits $(r', z', \theta', p_r', p_z', p_\theta')$ in Eq. (B.1) pass through the phase space point $(r - R_0, z, \theta, p_r, p_z, p_\theta)$ at time $t' = t$. Moreover, $p_r' = \gamma_b m v_r'$ and $p_z' = \gamma_b m v_z'$ for the nonrelativistic transverse motion described by Eq. (B.1). From Eq. (B.1), Hamilton's equations of motion $(d/dt')(\partial H/\partial P_r') = -\partial H/\partial r'$, $(d/dt')(\partial H/\partial P_z') = -\partial H/\partial z'$ and $d\theta'/dt' = \partial H/\partial P_\theta$, give

$$\gamma_b m \frac{d^2 r'}{dt'^2} = + \gamma_b m\omega_{c\theta}\frac{dz'}{dt'} + \omega_{cz}\frac{\delta P_\theta}{R_0} - \gamma_b m\omega_\beta^2 r', \tag{B.3}$$

$$\gamma_b m \frac{d^2 z'}{dt'^2} = -\gamma_b m \omega_{c\theta} \frac{dr'}{dt'} - \gamma_b m \omega_\beta^2 z' \ , \tag{B.4}$$

$$\frac{d\theta'}{dt'} = \omega_{cz} \left(1 - \frac{r'}{R_0} + \frac{\delta P_\theta}{\omega_{cz} \gamma_b^3 m R_0^2} \right) \ . \tag{B.5}$$

Simplifying Eqs. (B.3) and (B.4) gives the coupled oscillator equations

$$\frac{d^2}{dt'^2} r' - \omega_{c\theta} \frac{dz'}{dt'} + \omega_\beta^2 \left(r' - \frac{\omega_{cz}}{\gamma_b m \omega_\beta^2 R_0} \delta P_\theta \right) = 0 \ , \tag{B.6}$$

$$\frac{d^2}{dt'^2} z' + \omega_{c\theta} \frac{dr'}{dt'} + \omega_\beta^2 z' = 0 \ . \tag{B.7}$$

Introducing

$$\eta' = \left(r' - \frac{\omega_{cz}}{\gamma_b m \omega_\beta^2 R_0} \delta P_\theta \right) + i z', \tag{B.8}$$

Eqs. (B.6) and (B.7) can be combined to give

$$\frac{d^2}{dt'^2} \eta' + i \omega_{c\theta} \frac{d}{dt'} \eta' + \omega_\beta^2 \eta' = 0 \ , \tag{B.9}$$

which can be integrated to give

$$\eta' = \eta_+ \exp(i \omega_b^+ \tau) + \eta_- \exp(i \omega_b^- \tau) \ , \tag{B.10}$$

where $\tau = t' - t$, $\eta_\pm$ are constant complex amplitudes, and the frequencies $\omega_b^\pm$ are defined by Eq. (43)],

$$\omega_b^\pm = \frac{\omega_{c\theta}}{2} \left\{ 1 \pm \left[1 + \frac{4\omega_\beta^2}{\omega_{c\theta}^2} \right]^{1/2} \right\}. \tag{B.11}$$

Note from Eqs. (B.8) and (B.10) that the (r',z') motion is biharmonic in ω_b^+ and ω_b^-, and that r' and z' can be expressed as

$$r' = \frac{\omega_{cz}}{\gamma_b m \omega_\beta^2 R_0}\,\delta P_\theta + (\hat{r}'_+ \cos\omega_b^+\tau + \hat{r}'_- \cos\omega_b^-\tau) - (\hat{z}'_+ \sin\omega_b^+\tau + \hat{z}'_- \sin\omega_b^-\tau)\ , \tag{B.12}$$

$$z' = (\hat{z}'_+ \cos\omega_b^+\tau + \hat{z}'_- \cos\omega_b^-\tau) + (\hat{r}'_+ \sin\omega_b^+\tau + \hat{r}'_- \sin\omega_b^-\tau)\ . \tag{B.13}$$

The oscillation amplitudes $\hat{r}'_\pm$ and $\hat{z}'_\pm$ of course can be determined from the boundary condition that the particle trajectories (r',z',p'_r,p'_z) pass through $(r-R_0,z,p_r,p_z)$ at $\tau = t' - t = 0$. For a thin ring with $a \ll R_0$, we note that $|\hat{r}'_\pm|$, $|\hat{z}'_\pm| \ll R_0$.

Substituting Eq. (B.12) into Eq. (B.5) and integrating with respect to t', we obtain

$$\theta' = \theta + (\omega_{cz} - \mu\delta P_\theta/\gamma_b m R_0^2)\tau + (\text{small oscillations}), \tag{B.14}$$

where μ is defined by

$$\mu = \frac{\omega_{cz}^2}{\omega_\beta^2} - \frac{1}{\gamma_b^2}\ . \tag{B.15}$$

In Eq. (B.14), the small oscillatory terms (of order a/R_0) are biharmonic in $\omega_b^\pm$ and make negligibly small contributions in the frequency regime considered in the stability analysis in Sec. III. Depending on the sign of $\beta_b^2 - (1-f)$ and the size of γ_b and ω_{pb}/ω_{cz}, we note from Eq. (B.15) that μ can assume large positive or negative values.

DISTRIBUTION

	Copies
Commander	
Naval Research Laboratory	
Attn: Dr. Saeyoung Ahn	1
Dr. Wahab A. Ali	1
Dr. J. M. Baird	1
Dr. L. Barnett	1
Dr. O. Book	1
Dr. Jay Boris	1
Dr. K. R. Chu	1
Dr. Timothy Coffey	1
Dr. G. Cooperstein	1
Dr. A. Drobot	1
Dr. Richard Fernslor	1
Dr. H. Freund	1
Dr. M. Friedman	1
Dr. J. Golden	1
Dr. S. Goldstein	1
Dr. V. Granatstein	1
Dr. Robert Greig	1
Dr. Irving Haber	1
Dr. Richard Hubbard	1
Dr. Bertram Hui	1
Dr. Glenn Joyce	1
Dr. Selig Kainer	1
Dr. C. A. Kapetanakos	1
Dr. M. Lampe	1
Dr. Y. Y. Lau	1
Dr. W. M. Manheimer	1
Dr. Don Murphy	1
Dr. Peter Palmadesso	1
Dr. Robert Pechacek	1
Dr. Michael Picone	1
Dr. Michael Raleigh	1
Dr. M. E. Read	1
Dr. C. W. Roberson	1
Dr. J. D. Sethian	1
Dr. William Sharp	1
Dr. J. S. Silverstein	1
Dr. Philip Sprangle	1
Dr. Doug Strickland	1
Dr. C. M. Tang	1
Dr. N. Vanderplaats	1
Washington, DC 20375	

	Copies
Office of Naval Research	
Attn: Dr. Robert Behringer	1
1030 E. Green	
Pasadena, CA 91106	
Office of Naval Research	
Attn: Dr. T. Berlincourt	1
Dr. W. J. Condell	1
Department of the Navy	
Arlington, VA 22217	
Commander	
Naval Air Systems Command	
Attn: Dr. Wasneski	1
Department of the Navy	
Washington, DC 20361	
Commander	
Naval Sea Systems Command	
Attn: Dr. C. F. Sharn	1
Department of the Navy	
Washington, DC 20362	
Harry Diamond Laboratory	
Attn: Dr. H. E. Brandt	1
Dr. S. Graybill	1
2800 Powder Mill Road	
Adelphi, MD 20783	
U. S. Army Ballistic Research Laboratory	
Attn: Dr. D. Eccleshall	1
Aberdeen Proving Ground	
MD 21005	
Air Force Weapons Laboratory	
Attn: Dr. Ray Lemke	1
Kirtland Air Force Base	
Albuquerque, NM 87117	
Air Force Weapons Laboratory	
Attn: Dr. D. Straw	1
Kirtland AFB, NM 87117	

DISTRIBUTION (Cont.)

	Copies
U.S. Department of Energy	
Attn: Dr. T. Godlove	1
Dr. M. Month	1
Dr. J. A. Snow	1
Washington, DC 20545	
National Bureau of Standards	
Attn: Dr. Sam Penner	1
Bldg. 245	
Washington, DC 20234	
National Bureau of Standards	
Attn: Dr. Mark Wilson	1
Gaithersburg, MD 20760	
Defense Advanced Research Projects Agency	
Attn: Dr. J. Bayless	1
Dr. Robert Fossum	1
Dr. J. A. Mangano	1
LCOL W. Whitaker	1
1400 Wilson Blvd.	
Arlington, VA 22209	
Science Applications Inc.	
Attn: Dr. Richard E. Aamodt	1
934 Pearl St. Suite A	
Boulder, CO 80302	
Science Applications Inc.	
Attn: Dr. L. Feinstein	1
Dr. Robert Johnston	1
Dr. Douglas Keeley	1
Dr. John Siambis	1
5 Palo Alto Square	
Palo Alto, CA 94304	
Science Applications, Inc.	
Attn: Dr. A. W. Trivelpiece	1
San Diego, CA 92123	
Science Applications, Inc.	
Attn: Dr. Ron Parkinson	1
1200 Prospect Street	
P.O. Box 2351	
La Jolla, CA 92038	

	Copies
TRW	
Defense and Space Systems Group	
Attn: Dr. D. Arnush	1
Dr. M. Caponi	1
1 Space Park	
Redondo Beach, CA 90278	
Lawrence Livermore National Laboratory	
Attn: Dr. W. A. Barletta	1
Dr. R. Briggs	1
Dr. H. L. Buchanan	1
Dr. Frank Chambers	1
Dr. T. Fessenden	1
Dr. Edward P. Lee	1
Dr. James Mark	1
Dr. Jon A. Masamitsu	1
Dr. V. Kelvin Neil	1
Dr. R. Post	1
Dr. D. S. Prono	1
Dr. M. E. Rensink	1
Dr. Simon S. Yu	1
University of California	
Livermore, CA 94550	
Physics International Co.	
Attn: Dr. Jim Benford	1
Dr. S. Putnam	1
2700 Merced Street	
San Leandro, CA 94577	
Sandia Laboratories	
Attn: Dr. K. D. Bergeron	1
Dr. B. Epstein	1
Dr. S. Humphries	1
Dr. Tom Lockner	1
Dr. Bruce R. Miller	1
Dr. C. L. Olson	1
Dr. Gerold Yonas	1
Albuquerque, NM 87115	
La Jolla Institute	
Attn: Dr. K. Brueckner	1
Prof. N. M. Kroll	1
P.O. Box 1434	
La Jolla, CA 92038	

DISTRIBUTION (Cont.)

	Copies
Mission Research Corp. Attn: Dr. Neal Carron Dr. Conrad Longmire 735 State Street Santa Barbara, CA 93102	1 1
Mission Research Corp. Attn: Dr. B. Godfrey 1400 San Mateo Blvd, S.E. Suite A Albuquerque, NM 87108	1
McDonnell Douglas Corp. Attn: Dr. M. Greenspan Dr. J. Carl Leader P. O. Box 516 St. Louis, MO 63166	1 1
Los Alamos National Lab. Attn: Dr. Barry Newberger Dr. L. E. Thode Mail Stop 608 Los Alamos, NM 87544	1 1
Los Alamos Scientific Lab. Attn: Dr. H. Dreicer Dr. R. J. Faehl Los Alamos, NM 87544	1 1
Pulse Sciences, Inc. Attn: Dr. Sid Putnam 1615 Broadway, Suite 610 Oakland, CA 94612	1
National Science Foundation Attn: Dr. R. Hill Physics Division, #341 Washington, DC 20550	
W. J. Schafer Associates, Inc. Attn: Dr. Edward Cornet 1901 North Fort Myer Dr. Arlington, VA 22209	1
Austin Research Associates Attn: Prof. W. E. Drummond Dr. M. Lee Sloan Dr. James R. Thompson 1901 Rutland Drive Austin, TX 78758	1 1 1
Western Research Corporation Attn: Dr. Franklin Felber 8616 Commerce Avenue San Diego, CA 92121	1
Jaycor Attn: Dr. J. U. Guillory Dr. D. Tidman 205 S. Whiting Street Alexandria, VA 22304	1 1
Varian Associates Attn: Dr. Howard Jory 611 Hansen Way Palo Alto, CA 94303	1
Lawrence Berkeley Lab. Attn: Dr. Denis Keefe Dr. Hogil Kim Dr. Hong Chul Kim Dr. Kwang Je Kim Dr. L. J. Laslett Dr. G. R. Lambertson Dr. A. M. Sessler Dr. L. Smith 1 Cyclotron Road Berkeley, CA 94720	1 1 1 1 1 1 1 1
Stanford Linear Accelerator Center Attn: Dr. Philip Morton P.O. Box 4349 Stanford, CA 94305	1
AVCO - Everett Research Laboratory, Inc. Attn: Dr. Richard Patrick 2385 Revere Beach Pkwy Everett, MA 02149	1

DISTRIBUTION (Cont.)

	Copies
Oak Ridge National Lab	
Attn: Dr. J. A. Rome	1
Oak Ridge, TN 37850	
University of California at Los Angeles	
Attn: Prof. F. Chen	1
Dr. A. T. Lin	1
Dr. J. Dawson	1
Dr. C. S. Liu	1
Dr. Edward Ott	1
Los Angeles, CA 90024	
University of Maryland	
Attn: Dr. W. Destlar	1
Dr. C. S. Liu	1
Dr. Won Namkung	1
Dr. E. Ott	1
Prof. M. Reiser	1
Dr. Moon-Jhong Rhee	1
Dr. C. D. Striffler	1
College Park, MD 20742	
Columbia University	
Attn: Prof. P. Diament	1
Prof. S. Schlesinger	1
New York, NY 10027	
North Carolina State University	
Attn: Prof. W. Doggett	1
Dr. Jin Joong Kim	1
P. O. Box 5342	
Raleigh, NC 27650	
Massachusetts Institute of Technology	
Attn: Prof. George Bekefi	1
Dr. K. J. Button	1
Prof. R. Davidson	1
Dr. R. Temkin	1
77 Massachusetts Avenue	
Cambridge, MA 02139	

	Copies
University of California	
Attn: Dr. Gregory Benford	1
Dr. A. Fisher	1
Prof. N. Rostoker	1
Physics Department	
Irvine, CA 92717	
Yale University	
Attn: Dr. I. B. Bernstein	1
Dr. J. L. Hirshfield	1
Mason Laboratory	
400 Temple Street	
New Haven, CT 06520	
Cornell University	
Attn: Prof. H. Fleischmann	1
Prof. D. Hammer	1
Prof. R. V. Lovelace	1
Prof. J. Nation	1
Prof. R. Sudan	1
Ithaca, NY 14850	
University of Texas at Austin	
Attn: Dr. M. N. Rosenbluth	1
Institute for Fusion Studies	
RLM 11.218	
Austin, TX 78712	
Stevens Institute of Technology	
Attn: Prof. George Schmidt	1
Physics Department	
Hoboken, NJ 07030	
Dartmouth College	
Attn: Dr. John E. Walsh	1
Department of Physics	
Hanover, NH 03755	
Defense Technical Information Center	
Cameron Station	
Alexandria, VA 22314	12